Relationships of ground motion parameters and energy demands for SDOF and MDOF systems in RC buildings

Emrah MERAL

emrahmeral@osmaniye.edu.tr

Osmaniye Korkut Ata University: Osmaniye Korkut Ata Universitesi https://orcid.org/0000-0002-7635-0432

Research Article

Keywords: Ground motion parameter, intensity measures, reinforced concrete buildings, nonlinear time history analysis, input energy

Posted Date: June 20th, 2023

DOI: https://doi.org/10.21203/rs.3.rs-3029755/v1

Version of Record: A version of this preprint was published at Bulletin of Earthquake Engineering on March 25th, 2024. See the published version at https://doi.org/10.1007/s10518-024-01885-1.

Relationships of ground motion parameters and energy demands for SDOF and MDOF systems in RC buildings

Emrah Meral[1*]

[1*]Corresponding author, Ph.D., Department of Civil Engineering, Osmaniye Korkut Ata University, 80000 Osmaniye, Turkey, emrahmeral@osmaniye.edu.tr

ABSTRACT

This study aims to evaluate the correlation between ground motion parameters and energy demands of low-rise RC buildings without shear walls. Two regular 4- and 7-storey residential buildings are seismically designed to represent low-rise RC buildings. In order to establish the demands of single degree of freedom (SDOF) systems as well as multi degree of freedom (MDOF) systems, the dynamic features of "equivalent" SDOF systems are defined by using MDOF systems. The correlation of 20 ground motion parameters (GMPs) of 44 records with the energy demands obtained from a total of 176 nonlinear time history analyses is investigated for SDOF and MDOF systems within the scope of the study. The ground motion parameters (GMPs) have been taken as intensity measures (IMs) while values of maximum input energy are used as demand measure (DM) and these energy values are normalized with the masses of the buildings for cases where the buildings are evaluated together. Parameters related to acceleration and velocity are generally found to have better consequences than ones related to frequency and displacement. Velocity Spectrum Intensity (VSI) and Arias Intensity (I_a) have been obtained to have the highest correlation values as a single parameter. This study suggested new equations with combining multiple ground motion parameters for SDOF and MDOF systems to reflect damage potential better than a single parameter. The usage of combined multiple parameters achieves an evident enrichment of the correlation coefficients.

Keywords: Ground motion parameter, intensity measures, reinforced concrete buildings, nonlinear time history analysis, input energy

1. Introduction

Estimating earthquake damage is essential for the seismic performance of new buildings and the evaluation of existing structures taking into account the potential future earthquake hazard. Assessment of ground motion intensity measure (IM) and demand measure (DM) together enables to predict the damage risk of the earthquake. The ground motion parameters (GMPs) such as peak ground acceleration (PGA) and velocity (PGV), etc. have been taken as intensity measures (IMs) while the structural damage is quantified by demand measures (DMs) such as maximum roof drift ratio and input energy, etc. The GMPs present good correlation with DMs provides that the seismic performances of the structures are obtained properly. Therefore, investigations about the GMP that best reflects the seismic damage potential statistically continue today.

There are many studies shows that an interdependency between the behavior of structures and GMPs. Elenas (2000) emphasized that Park/Ang and DiPasquale/Çakmak as damage index have high correlation with spectral pseudo-acceleration (SA), medium correlation to PGV, peak ground displacement (PGD) and I_a, poor to medium correlation to effective peak acceleration (EPA) and poor correlation with PGA and ratio of peak acceleration to peak velocity (A_{max}/V_{max}). Elenas and Meskouris (2001) took into account demand measures (DMs) such as overall structural damage index (OSDI), maximum interstory drift ratio (MIDR) and maximum floor acceleration. They noted that SA have strong correlation while PGA occurs poor correlation with OSDI and MIDR. The I_a exhibits high correlation while A_{max}/V_{max} has low correlation with max. floor acceleration.

Akkar and Özen (2005) stated that the PGV has higher correlation when it is compared to PGA and PGV/PGA with spectral displacements on SDOF systems for short periods. PGV also reveals a more consistent correlation with inelastic displacement demands according to spectral acceleration (S_a). Yakut and Yılmaz (2008) concluded that housner intensity (HI), velocity spectrum intensity (VSI), and acceleration spectrum intensity (ASI) have the strongest correlation with maximum interstory drift ratio (MIDR) for structures with the period range of 0.1–2.5 s. PGA, VSI and characteristic intensity (I_c) are the highest correlated parameters for periods between 0.2–0.5 s while VSI, HI and S_a are the best parameters for periods between 0.5 and 1.1 s.

Cao and Ronagh (2014) investigated the relation between maximum inter-storey drifts, Park/Ang damage index and the characteristics of 1040 far-fault ground motion records. They indicated that PGD, PGV/PGA, displacement rms (D_{rms}), specific energy density (SED), predominant period (T_p) and mean period (T_m) exhibit poor correlations with the damage of structures. VSI is the best parameter of seismic damage potential, followed by HI and S_a. The findings also display PGA has weak correlation with the structural damage compared to other parameters. The overall structural damage index, as well as the maximum (MIDR) and average (AIDR) interstorey drift as structural damage states were correlated with GMPs by Kostinakis et al. (2015). According to the results, S_a, followed by VSI, PGV and HI correlate well with MIDR or AIDR as indicator of structural damage while PGV/PGA and D_{rms} are the least influential GMPs. Furthermore, the overall structural damage index demonstrates moderate or low correlation with most of the GMPs.

The correlation between nonlinear displacement drift demands and ground motion features was researched in accordance with number of storey and soil classes by Ozmen and Inel (2016). PGA and PGD have poor correlation with damage in comparison to the VSI, PGV and several different parameters as effective design acceleration (EDA) and I_c. The effective of GMPs on structural damage which was taken into account inter-story drift, roof drift and the Park/Ang index was examined utilizing regression coefficients by Massumi and Gholami (2016). They emphasized that VSI is the highest efficient parameter followed by the HI.

Damage potential of ground motion records was investigated using correlation coefficients between GMPs and displacement demands obtained from SDOF models and MDOF buildings that having diverse lateral strength capacities and periods depending on different soil properties by Palanci and Senel (2019). The

correlations of PGA, PGV and spectrum intensity (SI) are generally better than others while PGA, root mean square (RMS) of acceleration (A_{rms}), ASI have good correlations at low vibration periods of structures. In addition, correlation coefficients acquired from MDOF buildings are quite similar to the results of SDOF models. Kamal and Inel (2021) studied the correlation of GMPs with inelastic roof drift ratios of mid-rise RC frame buildings taking into account soil-structure interaction. HI has the greater correlation than all parameters while root mean square (RMS) of velocity (V_{rms}), VSI, SED, sustained maximum velocity (SMV), and PGV have good correlation. The least correlations are computed for the PGA and A95 parameters.

There are a limited number of studies that examine the relationship between GMPs and energy demand parameters as an indicator of structural damage. Riddell and Garcia (2001) performed a research to define GMPs that correlated well with input (E_I) and hysteretic (E_H) energy in SDOF systems. They concluded that peak ground motions parameters (PGA, PGV and PGD) show good correlation with energy dissipation in the long (displacement region) and short period (acceleration region) ranges of response spectra while HI is the best parameter in the intermediate period range (velocity region). Riddell (2007) evaluated the correlation between 23 ground motion intensity indices with four response variables such as elastic-inelastic deformation demands and input-hysteretic energy for SDOF systems. Although PGA and PGD exhibit better correlation with input and hysteretic energies in related to spectral regions, PGV has medium correlation. HI is the best parameter in the velocity region depending on correlation with both displacement and energy demands while it has poor and moderate correlation in the acceleration and displacement regions, respectively. In the short period range, I_a shows good correlation with energy demands.

Yang et al. (2009) carried out correlation analysis between 30 intensity measures (IMs) parameters and three demand measures (DMs) (maximum inelastic displacement, input and hysteretic energy) of SDOF systems. The acceleration-related parameters (I_c and I_a) are highly correlated with demand variables in the short-period range. The velocity-related parameter (PGV) exhibits good correlation in the medium and long period ranges. Koç (2017) examined effects of ground motion characteristics and structural features on distribution of seismic input energy depending on MDOF system using various types of ground motion records. According to the results of the analysis, a very high correlation is determined between the input energy (E_I) and the pseudo spectral velocity (PSV). Merter (2019) indicated that there is a good relationship between the maximum input energy demands of linear time history analysis and his proposed approach for SDOF systems. The suggested equation which contains $(PSV)_{max}$ and I_a correctly estimates the maximum elastic input energy.

In line with the studies in the literature, it is planned to conduct a study with distinctive characteristics. When the previous studies mentioned above are examined, it is understood that it is difficult to reach a definitive conclusion about the intensity of GMPs that represent the damage estimation of MDOF and SDOF systems. Most of these studies focus on different damage indexes, maximum interstory and roof drifts as a

damage indicator. On the other hand, the number of studies in which damage is associated with energy is limited. While past studies have generally been carried out on the SDOF system, ones related to MDOF system are usually based on a single structure or a two-dimensional (2D) frame building. In addition, either ground motion records or GMPs are considered in limited numbers for their works by researchers. Thence, this study examines the correlation of GMPs with input energy demands of low-rise RC buildings. It was scaled by selecting 44 real earthquake records in compliance with Turkish Building Earthquake Code (TBEC 2018). The 20 GMP based on 10 different seismic events was taken into account for each selected record. Maximum input energy is used as demand measurement and energy demands are normalized by the mass of the buildings. The relationship between roof displacements and input energy was also investigated for the considered buildings. Additionally, the distribution of hysteretic energy to storeys and structural elements was examined in scope of study.

2. Ground Motion Parameters

Summary definitions about considered the ground motion parameters are expressed in this section. More detailed information about these parameters can be found in the book called Geotechnical Earthquake Engineering by Kramer (1996). SeismoSignal (2022) software is used to obtain the values of the parameters within the scope of the study. A total of 20 ground motion parameters (GMPs) which are used to research the correlation between the parameters and the energy demands for SDOF and MDOF systems are described mainly about the content and the peak values of the ground motion records below:

- Peak Ground Acceleration (PGA): PGA is the simplest and is used widespread ground motion parameter to define severity of earthquake. Indicator of seismic excitations cannot be described by the PGA alone (Elenas, 1997) (Eq. (1)).

$$PGA = \max\left|a(t)\right| \tag{1}$$

- Peak Ground Velocity (PGV): Akkar and Özen (2005) demonstrated that PGV correlated better with SDOF deformation demands obtained from analyses according to other ground motion intensity measures (Eq. (2)).

$$PGV = \max\left|v(t)\right| \tag{2}$$

- Peak Ground Displacement (PGD): Elenas (Elenas, 2000), Elenas and Meskouris (2001) used this parameter for correlation with the structural damage (Eq. (3)).

$$PGD = \max\left|d(t)\right| \tag{3}$$

In the equations, a(t), v(t) and d(t) give the acceleration, velocity and displacement history of record.

- V_{max}/A_{max}: This V_{max}/A_{max} ratio has been utilized for near-field ground motions by researchers (Liao et al. 2001; Sucuoğlu et al. 1998; Sucuoğlu and Nurtuğ 1995; Zhu et al. 1988). (Eq. (4))

$$PGV / PGA = \frac{\max|v(t)|}{\max|a(t)|} \quad (4)$$

- Root-mean-square (RMS) of acceleration, velocity and displacement : These parameters are calculated by Eqs. (5-7) where t_t is the total duration of ground motion record.

$$a_{RMS} = \left[\frac{1}{t_t}\int_0^{t_t}\left[a(t)\right]^2 dt\right]^{1/2} ; \quad v_{RMS} = \left[\frac{1}{t_t}\int_0^{t_t}\left[v(t)\right]^2 dt\right]^{1/2} ; \quad d_{RMS} = \left[\frac{1}{t_t}\int_0^{t_t}\left[d(t)\right]^2 dt\right]^{1/2} \quad (5, 6, 7)$$

- Arias Intensity (I_a): I_a was proposed by Arias (1970) as a ground motion parameter related to the energy content of the ground motion and stated in Eq. (8). Some researchers emphasized that I_a correlates well with demand measures of structural performance, liquefaction and seismic slope stability (Travasarou et al. 2003).

$$I_a = \frac{\pi}{2g}\int_0^{t_t}\left[a(t)^2\right]dt \quad (8)$$

- Characteristic Intensity (I_c): The characteristic intensity (I_c) includes both the acceleration (see Eq.(5)) and duration-related parameters. It is expressed by Eq.(9).

$$I_c = \left(a_{RMS}\right)^{3/2}\sqrt{t_t} \quad (9)$$

- Cumulative Absolute Velocity (CAV): This parameter is defined with the Eq. (10) as the area under the absolute accelerogram. CAV discovered by Reed et al. (1988) in a study which sponsored by the Electric Power Research Institute. Cabanas et al. (1997) observed that CAV correlate well with damage.

$$CAV = \int_0^{t_t}|a(t)|dt \quad (10)$$

- A95 parameter: The acceleration level down which 95 percent of the I_a is contained. This parameter is defined by Sarma and Yang (1987) and it can be computed by Eq. (11).

$$A95 = 0.764 I_a^{\,0.438} \quad (11)$$

- Acceleration (ASI) and Velocity (VSI) Spectrum Intensity: ASI and VSI are calculated via spectral acceleration and velocity, respectively by Von Thun et al. (1988) in Eqs. (12,13) where ξ is damping ratio. S_a and S_v represent acceleration and velocity spectrum, respectively.

- $ASI = \int_{0.1}^{0.5} S_a(T)dT \ (\xi = 0.05)$; $VSI = \int_{0.1}^{2.5} S_v(T)dT \ (\xi = 0.05)$ (12, 13)

- Housner Intensity (HI): This parameter is suggested by Housner (1952) is given by Eq. (14). The VSI and HI are similar parameters, the only difference being that VSI is computed from the absolute velocity spectrum, whereas HI is based on the pseudo velocity spectrum.

$$HI = \int_{0.1}^{2.5} PSV(T)dT \ (\xi = 0.05)$$

(14)

- Specific Energy Density (SED): SED is determined by Eq. (15).

$$SED = \int_{0}^{t_t} [\mathrm{v}(t)]^2 dt \quad (15)$$

- Sustained Maximum Acceleration (SMA) and Velocity (SMV): SMA and SMV are identified as the third highest absolute value of acceleration and velocity in the time-history as proposed by Nuttli (Nuttli, 1979).
- Effective Design Acceleration (EDA): EDA corresponds to the peak acceleration value found after lowpass filtering the input time history with a cut-off frequency of 9 Hz (Reed et al. 1988).
- Predominant Period (T_p): T_p is the period at which the maximum spectral acceleration occurs in an acceleration response spectrum computed at 5% damping.
- Mean Period (T_m): T_m is the best simplified frequency content characterization parameter, being estimated with the Eq.(16), where C_i are the Fourier amplitudes, and f_i represent the discrete Fourier transform frequencies between 0.25 and 20 Hz (Rathje et al. 1998).

$$T_m = \frac{\sum C_i^2 / f_i}{\sum C_i^2} \quad (16)$$

Lots of parameters have been recommended to estimate the damage potential of strong ground motions as above. Some of these parameters are obtained from the ground motion records or the response spectra. Other parameters are calculated through equations. Ground motion parameters are divided into four classes: acceleration-related, velocity-related, frequency-related and displacement-related parameters. The parameters and their abbreviations used in this study are listed in Table 1.

Table 1 Definitions of the ground motion parameters

Type	Parameter	Identifier	Unit
Acceleration	Arias Intensity	I_a	m/s
	Characteristic Intensity	I_c	-
	Root Mean Square (RMS) of Acceleration	A_{rms}	g
	Sustained Maximum Acceleration	SMA	g
	Acceleration Spectrum Intensity	ASI	g.s
	Peak Ground Acceleration	PGA	g
	Effective Design Acceleration	EDA	g
	A95 parameter	A95	g
Velocity	Velocity Spectrum Intensity	VSI	m
	Housner Intensity	HI	m
	Cumulative Absolute Velocity	CAV	m/s
	Sustained Maximum Velocity	SMV	m/s
	Peak Ground Velocity	PGV	m/s
	Root Mean Square (RMS) of Velocity	V_{rms}	m/s
	Specific Energy Density	SED	m^2/s
Frequency	Predominant Period	T_p	s
	Ratio of Peak Velocity to Peak Acceleration	V_{max}/A_{max}	s
	Mean Period	T_m	s
Disp.	Peak Ground Displacement	PGD	m
	Root Mean Square (RMS) of Displacement	D_{rms}	m

3. Properties of Buildings and Modeling Approach

Two sets of building models with 4- and 7-storeys are designed to represent the low-rise buildings that form most of existing RC building stock in Turkey. The models as residential buildings are created depending on 2018 Turkish Building Earthquake Code (TBEC 2018). The building structural system consists of frames with beams and columns but no shear walls. The considered buildings have the same mold plan as shown in Fig. 1. The plan of 3D buildings is symmetrical in both X and Y directions. The building models have no irregularity in plan and elevation. The heights of all floors were assumed to be equal to 2.8 m along the building elevation. The beam dimensions are considered as 250x500 mm and 250x600 mm for 4-and 7- storey buildings, respectively. The column dimensions are selected as 400x400 mm and 500x500 mm for 4-and 7-storey buildings, respectively.

The unconfined, confined concrete and typical steel stress–strain model with strain hardening based on Mander et al. (1988) is applied in RC beam and column sections. When the expected concrete strength (f_{co}) is taken into account as 25 MPa for unconfined concrete, the concrete compressive strain (ε_{co}) corresponding to this value is 0.002. While confined concrete strength (f_{cc}) increases to 31.35 MPa thanks to the coating, the concrete compressive strain (ε_{cc}) becomes 0.004. In addition to these deformation values, the maximum compressive strain (ε_{cu}) in confined concrete is 0.0174. The yield strength (f_{sy}) of both longitudinal and transverse reinforcement is assumed to be 420 MPa for current study. As the elasticity modulus (E_s) of steel is taken as 200000 MPa, the yield strain (ε_{sy}) of the steel is calculated as 0.0021 and the strain (ε_{sh}) in steel is considered as 0.01 at onset of strain hardening. When the steel reaches maximum strength capacity (f_{su}) as 500 MPa, the maximum strain capacity (ε_{su}) of the steel takes the value as 0.09. The tensile-deformation relationships are defined for concrete and steel in Fig. 2. The longitudinal reinforcement ratios of the columns are chosen as approximately 1% for both 4- and 7-storey buildings. Peripheral stirrups as transverse reinforcements are used at 100mm spacing to reflect the ductile detailing compatible with the regulation. In addition to the peripheral stirrups, one crosstie with the same spacing as stirrups is considered in both directions for the column elements.

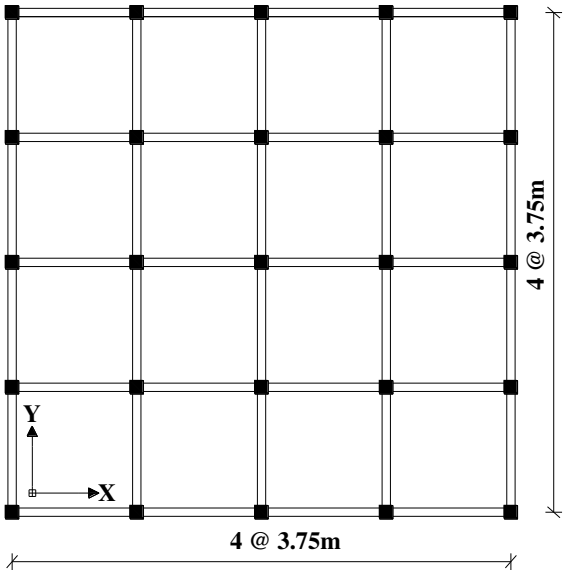

Fig. 1 Plan views of MDOF buildings

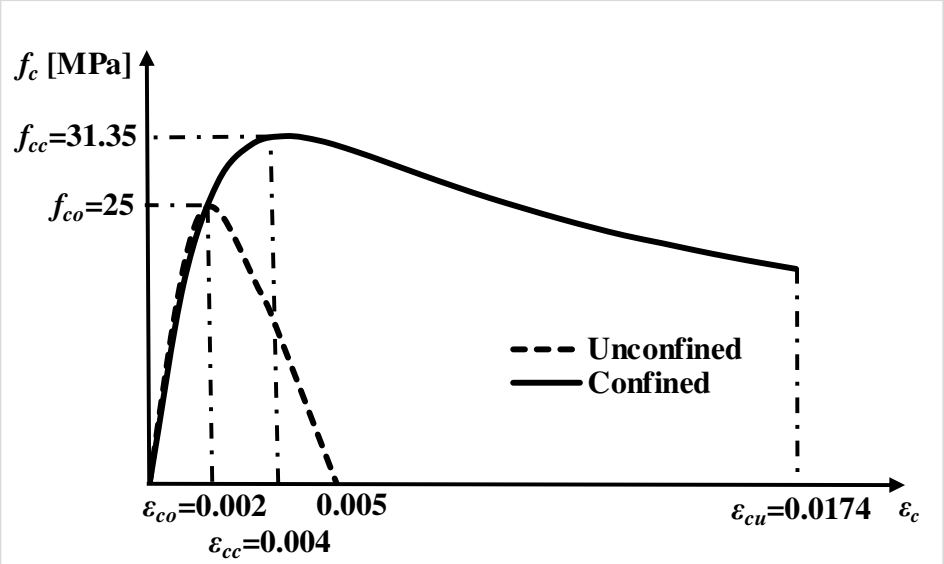

(a)

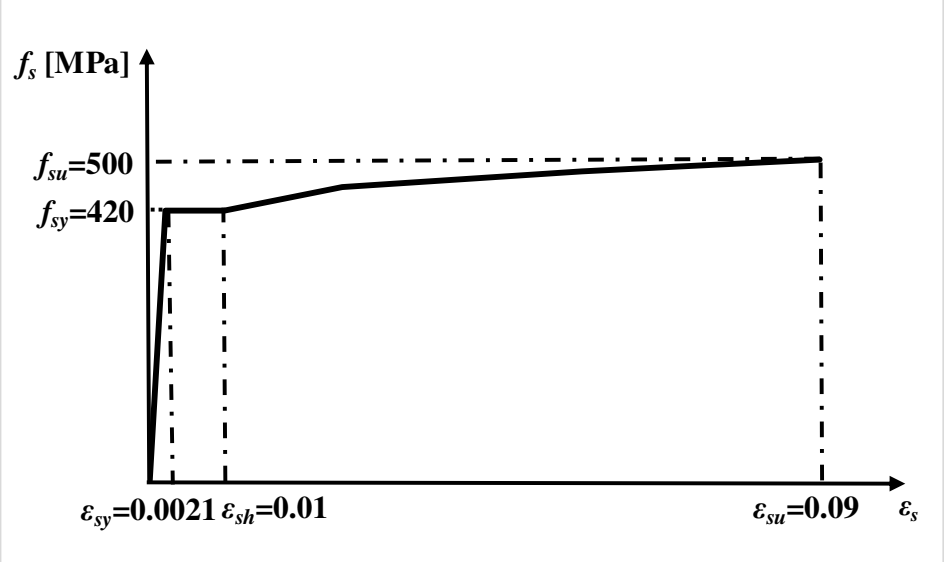

(b)

Fig. 2 Stress-strain plots: (a) Strength-strain relations for unconfined and confined concrete, (b) Strength-strain relationship for reinforcement steel

The slab thickness is taken into account as 150 mm in all floors of 4- and 7-storey building models. Since the load carrying system of the buildings consists of frames with beam and column members, slabs are not created as structural element during the design stage. The own weight of the slabs together with the coatings

and other loads on them are transferred to the beams around these slabs. It is assumed that there is an infill wall load of 4.5 kN/m on the other beams except for the beams on the roof floor. The other vertical loads in addition to the wall weight are considered as a dead load (g) of 3.75 kN/m^2 and a live load (q) of 2.0 kN/m^2 (1.5 kN/m^2 on upper floor) on the floors. The contribution to the lateral strength of infill walls is disregarded in building models for current study. Rigid diaphragms are applied separately at each floor level in order to transfer earthquake loads to the carrier elements in proportion to their stiffness. It should be noted that the mass of the structures was obtained by proportioning the weight values correspond to sum of the dead loads (g) and 30% of the live loads (q) to the gravitational acceleration.

The inelastic dynamic characteristics of MDOF buildings were converted into values of "equivalent" SDOF systems in order to analyze SDOF models. For this, the capacity curves reflecting the horizontal load carrying capacity of the buildings were obtained from the pushover analysis of the building models. Modal load pattern was used as horizontal load distribution in pushover analyses. The base shear is normalized by building weight while the roof displacement is normalized by building elevation to represent shear strength coefficient and roof drift ratio, respectively. The capacity curves were approximated with a bilinear curve in accordance with the principles specified in FEMA-356 (2000) guideline. Capacity curves of considered buildings are given in Fig. 3. Strength ratios at yield point (V_y/W) and post-yield stiffness ratios (plastic/elastic stiffness ratios) were calculated thanks to the idealized capacity curves (bilinear curves). The parameters reflecting the dynamic behavior of the structures are shown in Table 2. Structural response information such as dominant vibration periods and effective participating mass ratios depends on results of modal analysis. Moreover, since effective participating mass ratio of the first (dominant) vibration mode must be at least 0.70 to use pushover analysis according to the TBEC 2018, it is understood from the values in table that this condition is met.

Table 2 Structural features of building models

Building Models	**Period** (s)	**Effective Participating Mass Ratios** (%)	**Seismic Mass** (kNs^2/m)	V_y/W (%)	**Post-Yield Stiffness Ratios**
4-storey	0.50	82.4	985.09	0.21	0.042
7-storey	0.67	81.6	1953.56	0.16	0.051

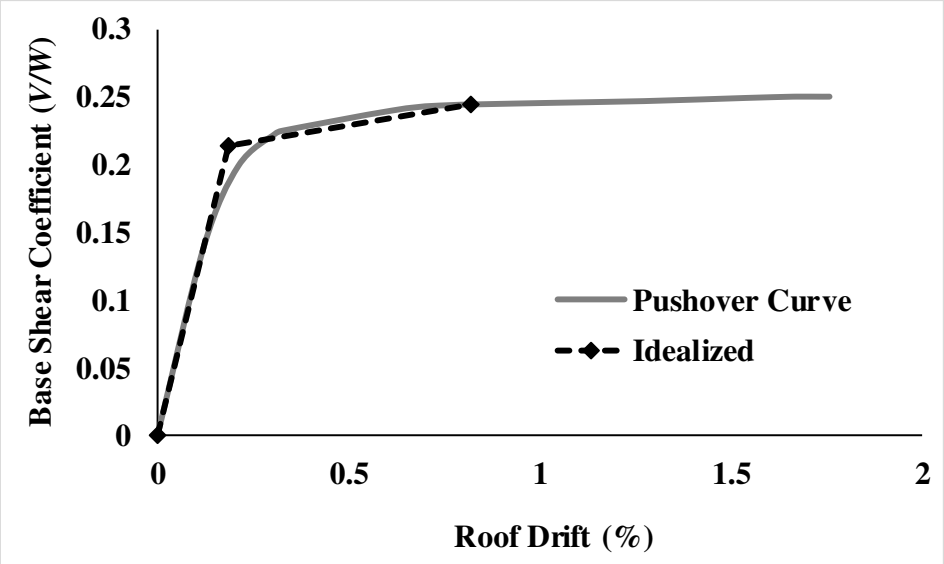

(a)

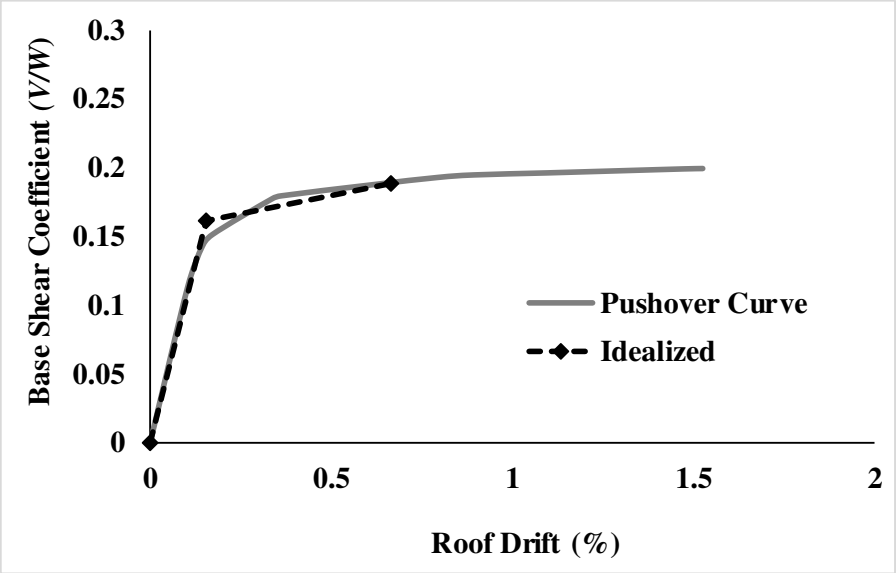

(b)

Fig. 3 Capacity curves: (a) for 4-storey and (b) for 7-storey building models

252

253 SAP2000 (2018) which is a general-purpose structural analysis program was used for modeling and
254 nonlinear analyses of structures. Beams and columns are modeled as nonlinear stick members using lumped
255 plastic behavior model by defining plastic hinges at both ends of beams and columns. The length of the plastic
256 deformation region is assumed to be equal half of the section depth of structural members in accordance with

TBEC 2018 and other regulations (e.g., ATC-40 1996 and FEMA-356). SAP2000 enables definition options of plastic hinges like user-defined hinge properties or auto (default) hinge properties explained in FEMA-356 and ASCE 41-13 (2014) which are used in current study to assign nonlinear behavior of frame elements. Automatic hinges request detailed information (material characteristics, dimensions of members, longitudinal and transverse reinforcement contents etc.) of the frame section property used by structural elements. The five points such as A, B, C, D, and E that define strength-displacement (as moment-rotation) relationship of a typical plastic hinge are shown in Fig. 4. The immediate occupancy (IO), life safety (LS) and collapse prevention (CP) are described as performance levels in FEMA-356 and ASCE 41-13. Bending rigidity of the beams and columns was multiplied by stiffness modification factors as 0.35 and 0.70 explained in TBEC 2018 to regard effective stiffness of the cracked section, respectively.

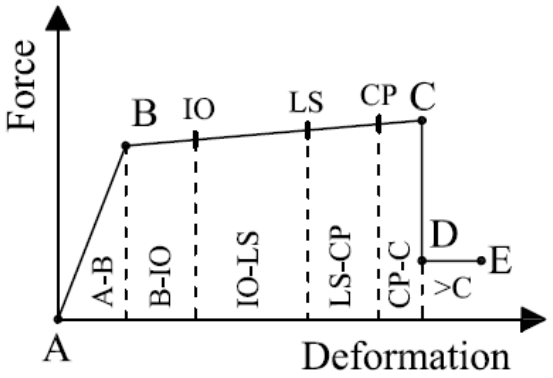

Fig. 4 Typical force-deformation relation for an auto plastic hinge

The direct integration method is chosen between two solution options as modal and direct integration for time history analysis of MDOF building models. A variety of widespread methods such as Chung and Hulbert, Collocation, Hilber-Hughes-Taylor, Wilson and Newmark are present for performing time history analysis with direct integration. The Newmark method with gamma (γ) = 0.5 and beta (β) = 0.25 is applied for nonlinear time history analyses. Mass and stiffness proportional coefficients are specified according to 5% damping by different periods for viscous proportional damping.

4. Selected ground motion records

For more reliable results, real ground motion records are used in nonlinear time history analyses. These records contain precise informations such as amplitude, frequency and duration about seismic events. They also reflect factors like soil properties and source distance that affect records. Because of these reasons, the selection and scaling of real records are very important in order to determine accurately the effects to be examined.

Two different reinforced concrete buildings representing low-rise structures are assumed to be located on

the soil class ZD defined in TBEC 2018 near Osmaniye Korkut Ata University in Osmaniye province of Turkey. The design (DD-2) and maximum (DD-1) earthquake levels, in which 10% and 2% probability of exceedance in 50 years, respectively, were taken into account to select the records. Two target response spectra were obtained to reflect the regional earthquake hazard by considering the coordinate of buildings, soil type and different earthquake levels. A total of 22 ground motion record sets from 10 different earthquakes compatible with target spectra were taken from the PEER (Pacific Earthquake Engineering Research) ground motion database (PEER 2019). Acceleration records in accordance with design and maximum acceleration spectra principles of TBEC 2018 were scaled by using simple scaling method for spectral matching between target spectra and spectrum of selected records via PEER. The resulting horizontal spectrum was generated by taking the square root of the sum of squares (SRSS) of the spectra of the scaled horizontal components belonging to each earthquake record pair. Ground motion components are scaled according to the rule that the average of the resultant spectra of the records should not be less than 1.3 times the target spectra in the period intervals specified in TBEC 2018. Resultant spectra related to 22 ground motion record sets, mean of resultant spectra and target spectra curve amplified with 1.3 coefficient for design (DD-2) and maximum (DD-1) earthquake levels are given in Fig. 5. Although the resultant spectra of selected records for especially periods of considered building models have spectral acceleration values in a wide band range, it is understood from the figure that average of these spectra is quite compatible with the 1.3 times target spectra. The features of the selected records and their scale factors are seen in Table 3. While the earthquake magnitudes (M_w) changed between 6.2 and 7.2, the distances were limited between 5 and 25 km. The shear wave velocity (V_{s30}) was chosen between 180 and 360 m/s to reflect the ZD soil class per TBEC 2018. Scaling coefficients sensibly range from 0.84 to 1.89 and 1.40 to 3.16 for design (DD-2) and maximum (DD-1) earthquake levels, respectively. The both horizontal components are scaled with the same scaling factors. Number of earthquake record sets should be at least 11 and number of record pairs to be selected from same earthquake shall not exceed three for time history analysis in accordance with TBEC 2018. The aforementioned circumstances in the regulation were taken into account in the selection and scaling of the ground motion records.

As the effective time of the ground motion increases, more energy input is expected to the structure. The most important difference of the energy parameters from other variables (base shear force and roof displacement etc.) is that they are not obtained as an instantaneous maximum value, they are calculated by summing the effects that occur during the ground motion. Many definitions such as “bracketed duration”, “uniform duration” and “significant duration” which vary according to the measured value have been made in order to determine the effective duration of the earthquake (Fahjan 2008). The parameter used in the calculation of the significant duration, which shows the time it takes for the energy in the acceleration record to be discharged, is Arias intensity (I_a), which indicates the amount of energy in the record. The curve showing the change of Arias Intensity (I_a) over time as a percentage is expressed as “Husid Plot”. The time between 5%

and 95% occurrence of Arias Intensity (I_a) over this curve is defined as "significant duration". The effective duration (t_e) of the records used in the study was determined with significant duration and added to Table 3. Fig. 6 shows the effective duration for Kobe-abn090 ground motion record. The effective duration of the record, which has a total recording time of 140 s, is calculated approximately as 56 s by the time difference (t_2-t_1).

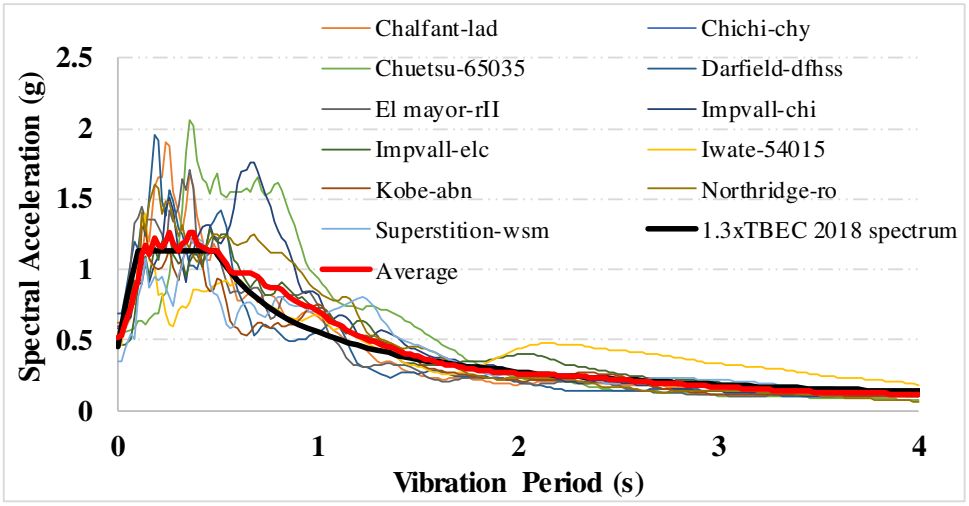

(a)

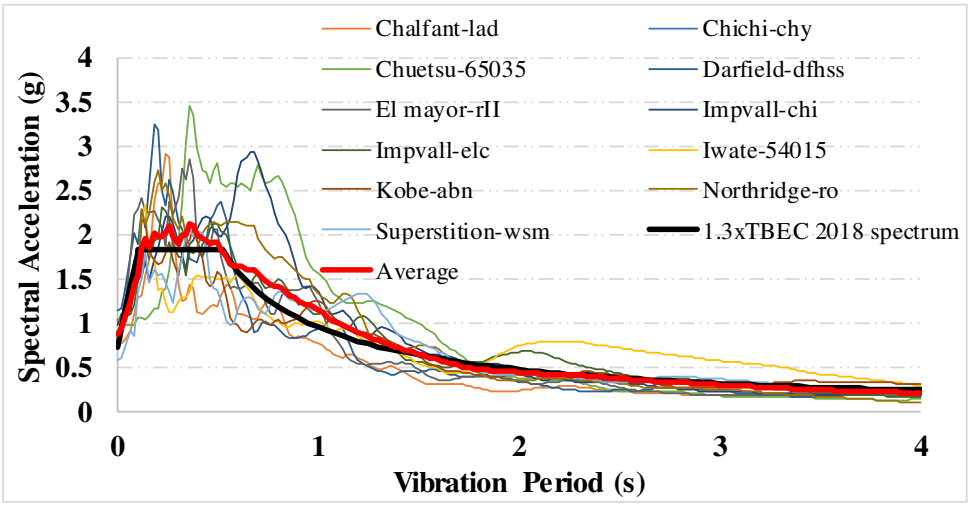

(b)

Fig. 5 The resultant spectra of scaled earthquake record sets for 5% damping: (a) for DD-2 and (b) for DD-1 earthquake levels

Table 3 Characteristics of ground motion records used in current study

No	Earthquake	Record	Station	Scale Factor (DD-2)	Scale Factor (DD-1)	Date	Magnitude	V_{s30} (m/s)	*Rjb* (km)	*Rrup* (km)	*te* (s)
1	Chalfant Valley	lad180	Bishop - LADWP South St	1.83	3.06	21.07.1986	6.2	303.47	6.09	6.09	17.18
2		lad270									
3	Chi-Chi	chy101e	Chy101	1.82	3.05	20.09.1999	6.2	258.89	7.29	7.29	18.44
4		chy101n									
5	Chuetsu	65035ew	Shiura Nagaoka	1.74	2.91	16.07.2007	6.8	336.93	14.38	17.17	25.85
6		65035ns									
7	Darfield	dfhss17e	Dfhs	0.98	1.64	04.09.2010	7.0	344.02	13.03	13.03	21.75
8		dfhss73w									
9	El Mayor	rii000	RIIto	0.84	1.40	04.04.2010	7.2	242.05	5.59	10.05	26.24
10		rii090									
11	Imperial Valley	chi012	Chihuahua	1.56	2.62	15.10.1979	6.5	242.05	24.85	24.85	24.26
12		chi282									
13	Imperial Valley	elc180	El Centro Array #9	1.32	2.21	15.10.1979	6.5	213.44	21.62	21.67	24.20
14		elc270									
15	Iwate	54015ew	Iwadeyama	1.04	1.74	14.06.2008	6.9	345.55	10.61	20.17	15.45
16		54015ns									
17	Kobe	abn000	Abeno	1.89	3.16	16.01.1995	6.9	256.00	20.77	20.78	56.39
18		abn090									
19	Northridge	ro3000	Sun Valley - Roscoe Blvd	1.19	1.99	17.01.1994	6.7	320.93	13.70	13.71	16.74
20		ro3090									
21	Superstition Hills	wsm090	Westmorland Fire Sta	1.28	2.14	24.11.1987	6.5	193.67	11.86	11.86	23.52
22		wsm180									

*Rjb** is Joyner-Boore distance defined as the closest horizontal distance to rupture plane (as epicentral distance)

*Rrup** is the closest distance to the rupture plane

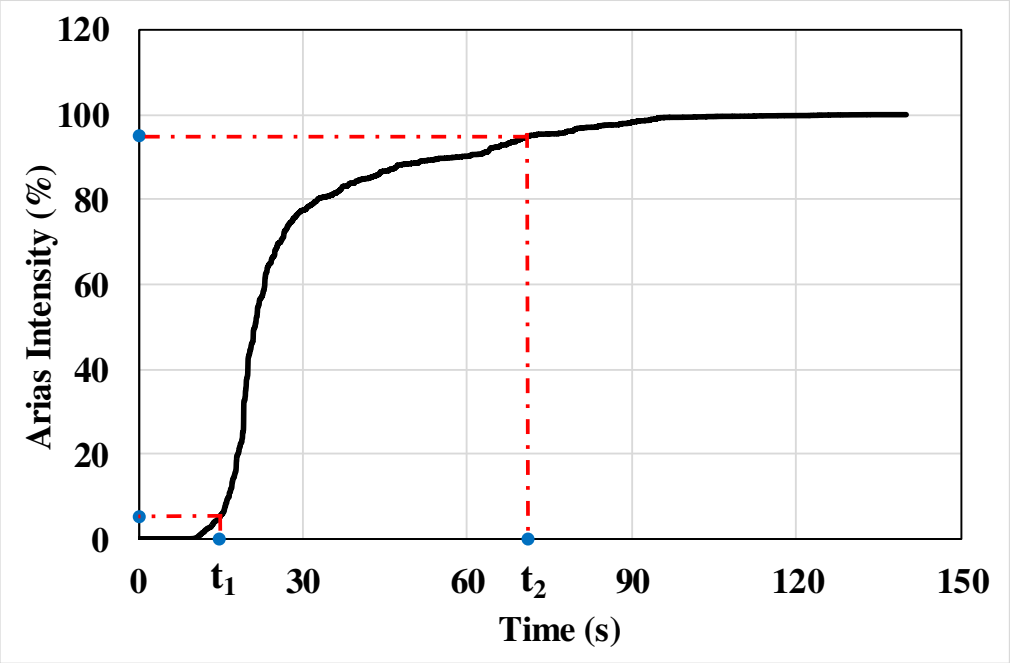

Fig. 6 Determination of significant duration for Kobe-abn090 record using Husid Plot

5. Energy-based design

Energy-based structural computation is a design method that investigates the distribution of the energy entering the building with strong ground motion to the structural elements and the consumption of this energy by the structural members. In order to mention about the energy phenomenon and energy-related parameters in building systems, equation of motion of the SDOF system should be considered at first. The seismic response of the SDOF system subjected to horizontal ground motion is expressed by the general dynamic equation of motion (Eq. (17)).

$$m\ddot{u} + c\dot{u} + ku = -m\ddot{u}_g(t) \tag{17}$$

where m, c and k represent mass, damping and stiffness, respectively. ü, u̇ , u and $\ddot{u}_g$ are acceleration, velocity, displacement and acceleration of strong ground motion, respectively. As a result of integrating Eq. (17) with respect to displacement, the general energy equation is obtained by Eq. (18).

$$\int_0^{u(t)} m\ddot{u}(t)du + \int_0^{u(t)} c\dot{u}(t)du + \int_0^{u(t)} ku(t)du = -\int_0^{u(t)} m\ddot{u}_g(t)du \tag{18}$$

The energy equation is easily related to the duration of the ground motion by writing du=u̇ dt in Eq. (18), and the integrals are expressed in terms of time by Eq. (19).

$$\int_0^t m\ddot{u}(t)\dot{u}dt + \int_0^t c\dot{u}(t)\dot{u}dt + \int_0^t ku(t)\dot{u}dt = -\int_0^t m\ddot{u}_g(t)\dot{u}dt \quad (19)$$

The input energy (E_I) caused by the earthquake is consumed by various components in structural systems. These components can be assumed as responses to the effect of the input energy on the building. The associated components; it is defined as the kinetic energy (E_K) related to the mass, the damping energy (E_D) related to the damping ratio, and the total energy (E_A) consumed in elastic and plastic behavior (Eq. (20)).

$$E_K + E_D + E_A = E_I \quad (20)$$

The elastic strain energy (E_S) and plastic strain energy (E_H) (non-recoverable hysteretic energy) which are the two components of the total energy (E_A) can be written separately in Eq. (21).

$$E_K + E_D + \left[E_S + E_H\right] = E_I \quad (21)$$

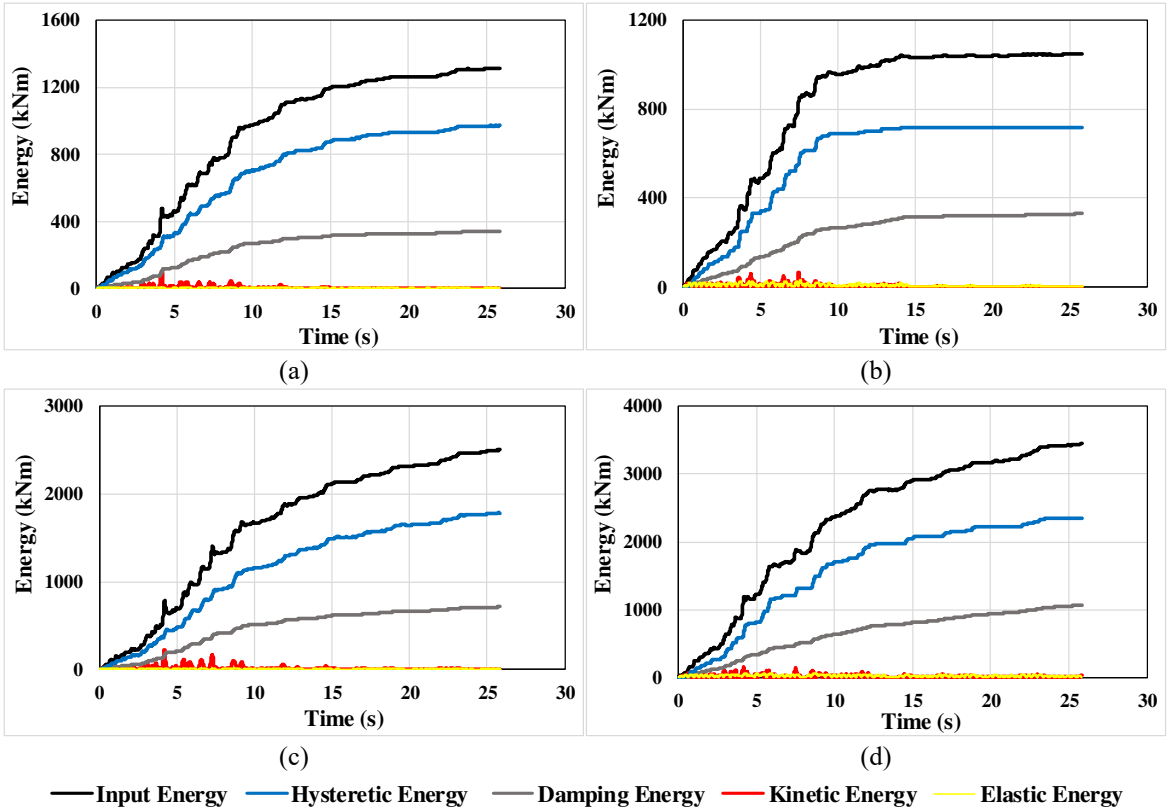

Fig. 7 The variation of energy parameters with time for Chuetsu-65035ew record: (a) for 4-storey model with SDOF, (b) MDOF, (c) for 7-storey model with SDOF and (d) MDOF

Samples of energy curves for SDOF and MDOF systems of 4- and 7- storey buildings are given in Fig. 7

in order to see energy changes for Chuetsu-65035ew record at design earthquake (DD-2) level. It is understood from the figure that the elastic (E_S) and kinetic (E_K) energy constitute much less of the input energy (E_I) than the hysteresis (E_H) and damping (E_D) energy. The energy in the structure is consumed mostly as hysteresis energy, followed by damping energy. The hysteresis and damping energy show a similar trend to the input energy, while other energies are separated from them. Based on figures, the energy amounts obtained in 4-storey model with SDOF are higher according to MDOF system, while the energy values of 7-storey model with SDOF are lower in comparison with the MDOF system. In terms of the number of storeys, the amount of energy calculated for the 7-storey model is higher than the 4-storey model.

6. Correlation coefficient

Correlation analysis; it is a statistical method that provides information about the relationship between variables, the direction (like positive and negative) and severity of this relationship. While the mathematical expression of the intercourse between two or more variables is determined by regression analysis, the direction and degree of the relation are examined by correlation analysis. The correlation coefficient is an indicator that reveals whether there is a linear relationship between two variables. In other words, it shows whether the changes in the variables affect each other. The value of the correlation coefficient ranges from -1 to +1. If the result is +1, it indicates that there is a strong positive relationship between the two variables and if the result is -1, it shows that there is a strong negative relationship. As the correlation coefficient approaches 0, the degree of the relationship decreases, while zero demonstrates that there is no linear relationship between the two variables. The degree of dependence between the variables depending on the correlation coefficients is detailed in Table 4. Determination coefficient is used to interpret how much of the observed variability in one variable is explained by the other variable and it is equal to the square of the correlation coefficient. The correlation coefficient is denoted by R, while the determination coefficient is expressed as R^2. The correlation coefficient between two variables X and Y is given by Eq. (22):

$$R(X,Y)=\frac{\sum_{i=1}^{N}(X_i-\bar{X})(Y_i-\bar{Y})}{\sqrt{\sum_{i=1}^{N}(X_i-\bar{X})^2\sum_{i=1}^{N}(Y_i-\bar{Y})^2}} \tag{22}$$

where $\bar{X}$ and $\bar{Y}$ are the average values of X_i and Y_i respectively, and N is the number of couple of values (X_i, Y_i) in the equation.

Table 4 Degrees of relationship corresponding to the correlation range

Correlation Range	Relation Level
-0.25 − -0.00 and 0.00 − 0.25	very weak
-0.49 − -0.26 and 0.26 − 0.49	weak
-0.69 − -0.50 and 0.50 − 0.69	middle
-0.89 − -0.70 and 0.70 − 0.89	high
-1.00 − -0.90 and 0.90 − 1.00	very high

7. Discussion of results

The energy and displacement values were obtained from nonlinear time history analyzes of 4- and 7- storey buildings for SDOF and MDOF systems. Input energy, hysteretic energy, distribution of hysteretic energy to floors and structural elements calculated from analyzes with design (DD-2) and maximum (DD-1) ground motions were examined. The relationship between input energy and hysteretic energy is investigated separately according to selected ground motion records. In addition, the intercourse between roof drift and input energy has been researched in terms of SDOF and MDOF systems.

7.1 Energy

Ground motion records used in the nonlinear analyzes revealed inelastic behaviors in SDOF and MDOF models and hysteretic energy which is an indicator of damage was released. Hysteretic energy is consumed by the formation of plastic hinges in structural members for MDOF buildings. Hysteretic energy is generated in SDOF systems using period, strength ratio, post-yield stiffness ratio by nonlinear time history analysis of SDOF models. The acceleration values of the maximum ground motions are higher than the design earthquakes increases the intensity of the records and the structural input energy.

The input energy is significantly affected by the characteristics of the ground motions. Table 5 shows that the smallest and biggest energies are found in the Chichi-chy101n and Chuetsu-65035ew records for two earthquake levels in the 4-storey model, respectively. In the 7-storey building, the highest values are calculated for the Chuetsu-65035ew at both SDOF and MDOF, while the lowest results are given in Table 6, where Chichi-chy101n for SDOF and Iwate-54015ns for MDOF. The acceleration values and effective duration of the Chuetsu-65035ew record are higher than the other two records provided an important increment in both hysteretic energy (E_H) and input energy (E_I). However, no parallel trend is observed between the increase-decrease of energy amount and the E_H/E_I ratios.

In order to understand the effects of earthquake levels on the analysis results, the hysteretic energy (E_H) and input energy (E_I) values of the maximum earthquakes were divided by the design ground motion values. In addition, the SDOF values were normalized with MDOF ones to reveal the changes of one- and three-dimensional modeling on the results. The E_H and E_I mean values of the maximum records for the SDOF

system are approximately 2.8 times the design data. The DD-2/DD-1 ratio is calculated as 3.35 and 2.83 for E_H and E_I, respectively, in the 4-storey model for the MDOF system, while it is 2.86 and 2.49 for the 7-storey building. While the difference between the energy ratios in terms of the earthquake levels is the same for the 4- and 7-storey models in the SDOF system, lower values are obtained in the 7-storey building model for the MDOF.

For the 4-storey model of the SDOF system, the E_H and E_I values of the design earthquakes are 37% and 10% more than the MDOF, while they are 15% and 9% higher per the results based on the maximum records. When the comparison is made for 7-storey building in the same way, 9% increase for E_H and 8% decrease for E_I is calculated for design records. According to the data of maximum earthquakes, 7% and 4% increment are obtained for E_H and E_I, respectively. Depending on the findings, it can be said that there is an increasing trend for both 4- and 7- storey models, except for the E_I value of the 7-storey model for the SDOF/MDOF ratio. If it is wanted to evaluate the difference between the models in terms of storey number, the E_H and E_I values for the design earthquakes of the 7-storey model for the MDOF system are 2.40 and 2.32 times, respectively, the 4-storey building, while it is approximately 2 times for maximum earthquakes. It should be kept in mind that it ensures the energy to be high due to the mass of the 7-storey building is approximately 2 times higher than the 4-storey building, which affects the input energy more than other structural features (period, stiffness and ductility, etc.).

Many researchers have attempted to obtain stable trends for the ratio of hysteretic energy to input energy (E_H/E_I) (Benavent-Climent et al. 2010; Dindar et al. 2015; Fajfar and Vidic 1994; Khashaee et al. 2003; Okur and Erberik 2014). The E_H/E_I ratio for SDOF systems is calculated as 0.72 and 0.71 according to average values, respectively, in 4- and 7-storey buildings, which shows that similar conclusions are obtained with the E_H/E_I=0.7 value suggested by Fajfar and Vidic (1994), Okur and Erberik (2014). According to the analysis results with design earthquakes considering MDOF systems, the E_H/E_I ratio is 0.55 for both 4- and 7-storey buildings, which is lower than the SDOF results. The value of 0.67 calculated with the maximum ground motions reveals that the E_H/E_I data of the MDOF approach the SDOF as the earthquake level increases. Although the E_H/E_I ratio has different values for SDOF and MDOF systems, it has been observed that it has almost the same average values for 4- and 7-storey models.

The input energy is affected by both the structural features and the characteristics of the ground motions. Therefore, as the ground motion and structural system change, it is clear that there will be differences in parameters such as input energy and hysteretic energy. Structural damage occurs in direct proportion to hysteretic energy. In the building where damage started to occur, they consume hysteretic energy by exhibiting inelastic behavior at the end regions of the structural elements. Hence, it can be expected that the damage occurrence will vary in 4- and 7-storey buildings depending on the structural features with the selected earthquakes. It is understood from Fig. 8 that majority of the hysteretic energy is consumed in the first three

and five storeys for 4- and 7-storey buildings, respectively. The storeys except for the aforementioned storeys exhibited generally elastic behavior. The increase in the earthquake level for both building groups does not create any significant difference in the distribution of hysteretic energy.

Table 5 Energy values of the 4-storey building model

Earthquakes	SDOF						MDOF					
	DD-2			DD-1			DD-2			DD-1		
	E_H (kNm)	E_I (kNm)	E_H/E_I	E_H (kNm)	E_I (kNm)	E_H/E_I	E_H (kNm)	E_I (kNm)	E_H/E_I	E_H (kNm)	E_I (kNm)	E_H/E_I
Chalfant-lad180	290.84	387.17	0.75	814.10	1083.74	0.75	233.98	365.23	0.64	710.67	989.61	0.72
Chalfant-lad270	217.89	311.78	0.70	609.91	872.73	0.70	205.95	360.44	0.57	584.59	902.91	0.65
Chichi-chy101e	241.82	321.54	0.75	676.84	899.97	0.75	121.26	253.68	0.48	421.97	678.11	0.62
Chichi-chy101n	156.61	212.77	0.74	438.34	595.54	0.74	93.63	180.33	0.52	382.71	579.44	0.66
Chuetsu-65035ew	971.07	1315.88	0.74	2718.18	3683.37	0.74	717.71	1049.87	0.68	2613.07	3463.31	0.75
Chuetsu-65035ns	750.78	1052.35	0.71	2101.56	2945.71	0.71	701.78	1022.46	0.69	2067.48	2822.30	0.73
Darfield-dfhss17e	387.96	519.39	0.75	1085.89	1453.76	0.75	201.27	440.39	0.46	815.81	1256.15	0.65
Darfield-dfhss73w	480.99	670.02	0.72	1346.29	1875.38	0.72	463.16	814.90	0.57	1290.16	1919.79	0.67
El mayor-r000	333.29	465.36	0.72	932.93	1302.61	0.72	254.51	521.06	0.49	860.89	1368.89	0.63
El mayor-r090	414.89	589.22	0.70	1161.33	1649.29	0.70	327.32	640.52	0.51	1208.60	1847.51	0.65
Impvall-chi012	667.84	916.74	0.73	1869.37	2566.08	0.73	572.00	869.61	0.66	1706.39	2394.28	0.71
Impvall-chi282	767.74	1088.49	0.71	2149.01	3046.82	0.71	666.82	928.75	0.72	2120.54	2851.87	0.74
Impvall-elc180	575.61	789.12	0.73	1611.20	2208.83	0.73	362.98	673.74	0.54	1260.97	1855.77	0.68
Impvall-elc270	412.06	578.05	0.71	1153.40	1618.03	0.71	273.44	537.65	0.51	1002.17	1539.82	0.65
Iwate-54015ew	418.08	551.61	0.76	1170.22	1543.99	0.76	302.11	474.99	0.64	938.05	1296.76	0.72
Iwate-54015ns	262.44	342.00	0.77	734.58	957.27	0.77	73.76	190.51	0.39	364.93	582.02	0.63
Kobe-abn000	339.17	480.59	0.71	949.41	1345.29	0.71	204.59	442.59	0.46	730.24	1184.28	0.62
Kobe-abn090	266.21	397.00	0.67	745.20	1111.31	0.67	146.08	398.68	0.37	519.10	977.72	0.53
Northridge-ro3000	361.28	495.41	0.73	1011.18	1386.61	0.73	348.81	598.37	0.58	1101.52	1578.99	0.70
Northridge-ro3090	485.90	689.19	0.71	1359.97	1928.96	0.71	375.14	563.49	0.67	1159.03	1641.95	0.71
Superstition-wsm090	223.84	302.20	0.74	626.51	845.82	0.74	94.11	268.60	0.35	418.85	724.61	0.58
Superstition-wsm180	491.03	711.49	0.69	1374.33	1991.40	0.69	191.72	367.66	0.52	978.97	1382.27	0.71
Mean	432.61	599.43	0.72	1210.90	1677.84	0.72	315.10	543.80	0.55	1057.12	1538.11	0.67

463 Table 6 Energy values of the 7-storey building model

Earthquakes	SDOF						MDOF					
	DD-2			DD-1			DD-2			DD-1		
	E_H (kNm)	E_I (kNm)	E_H/E_I	E_H (kNm)	E_I (kNm)	E_H/E_I	E_H (kNm)	E_I (kNm)	E_H/E_I	E_H (kNm)	E_I (kNm)	E_H/E_I
Chalfant-lad180	635.09	855.77	0.74	1777.71	2395.42	0.74	585.43	909.50	0.64	1620.60	2271.03	0.71
Chalfant-lad270	379.15	553.64	0.68	1061.29	1549.73	0.68	204.76	420.35	0.49	1044.89	1548.24	0.67
Chichi-chy101e	612.00	843.67	0.73	1712.95	2361.38	0.73	191.77	436.11	0.44	760.65	1192.60	0.64
Chichi-chy101n	340.18	450.48	0.76	952.13	1260.87	0.76	273.78	521.61	0.52	774.96	1241.32	0.62
Chuetsu-65035ew	1782.76	2503.52	0.71	4990.22	7007.76	0.71	2348.90	3447.07	0.68	5544.52	7682.68	0.72
Chuetsu-65035ns	1400.81	1980.93	0.71	3921.10	5544.97	0.71	1952.75	2998.73	0.65	4591.44	6480.30	0.71
Darfield-dfhss17e	869.57	1184.02	0.73	2433.92	3314.04	0.73	547.19	1072.37	0.51	1986.09	2929.46	0.68
Darfield-dfhss73w	695.02	1009.60	0.69	1945.36	2825.86	0.69	550.42	1113.57	0.49	1815.95	2835.58	0.64
El mayor-r000	610.81	857.67	0.71	1709.73	2400.71	0.71	430.37	889.41	0.48	1505.46	2385.25	0.63
El mayor-r090	616.58	901.09	0.68	1725.89	2522.27	0.68	735.82	1331.79	0.55	2057.75	3190.70	0.64
Impvall-chi012	1232.77	1706.42	0.72	3450.66	4776.49	0.72	1446.73	2197.84	0.66	3462.21	4907.45	0.71
Impvall-chi282	1351.89	1936.30	0.70	3784.09	5419.95	0.70	1817.72	2604.76	0.70	4333.62	5935.95	0.73
Impvall-elc180	1003.10	1444.15	0.69	2807.78	4042.33	0.69	980.04	1636.27	0.60	2782.93	3980.07	0.70
Impvall-elc270	754.42	1071.51	0.70	2111.70	2999.28	0.70	490.19	963.94	0.51	1657.69	2537.84	0.65
Iwate-54015ew	932.92	1258.57	0.74	2611.28	3522.77	0.74	586.18	953.96	0.61	1844.76	2581.11	0.71
Iwate-54015ns	779.67	1088.76	0.72	2182.34	3047.49	0.72	157.67	357.88	0.44	753.23	1117.39	0.67
Kobe-abn000	642.09	922.70	0.70	1797.37	2582.85	0.70	428.24	823.17	0.52	1638.90	2523.88	0.65
Kobe-abn090	626.47	928.87	0.67	1753.64	2600.14	0.67	153.77	488.11	0.32	1003.57	1785.76	0.56
Northridge-ro3000	585.64	820.18	0.71	1639.13	2295.58	0.71	689.71	1186.97	0.58	1882.52	2737.42	0.69
Northridge-ro3090	993.52	1408.97	0.71	2780.76	3943.56	0.71	926.32	1379.16	0.67	2513.43	3537.30	0.71
Superstition-wsm090	486.45	664.19	0.73	1361.52	1859.00	0.73	287.65	647.94	0.44	1184.91	1836.09	0.65
Superstition-wsm180	873.27	1291.81	0.68	2444.19	3615.63	0.68	843.53	1396.10	0.60	2831.61	3925.08	0.72
Mean	827.46	1167.40	0.71	2316.13	3267.64	0.71	755.86	1262.57	0.55	2163.26	3143.75	0.67

464

465 As a requirement of the capacity design approach, with the principle of "strong column-weak beam", a
466 significant part of the earthquake energy is expected to be consumed by the plastic hinges of the beams. The
467 formation of plastic hinges primarily at the beam ends ensures that the structure system behaves ductile.
468 Thanks to the ductile behavior, redistribution occurs and load transfer happens between neighboring elements.
469 Thus, sudden collapse mechanisms are prevented while plastic hinges are formed in more structural elements.
470 At the same time, more earthquake energy is absorbed when ductile damage occurs. As can be seen from Fig.
471 9, the majority of the hysteretic energy occurs in the beams relative to the columns is an indication of
472 compliance with the relevant capacity design principle. For design earthquakes, approximately 90% and 95%

of the hysteretic energy was generated in the beams of 4- and 7-storey buildings, respectively. By using the maximum earthquakes, the hysteretic energy consumed in the columns was increased by 10% and 5% for the 4- and 7-storey models. Since the spectral acceleration values corresponding to the period of the 4-storey building are generally higher on the spectrum of earthquakes selected in accordance with the response spectra, the 4-storey building was exposed to more earthquake loads on a floor basis. Therefore, since the columns of the 4-storey building are more damaged than the 7-storey model, the share of hysteretic energy in consumption has increased.

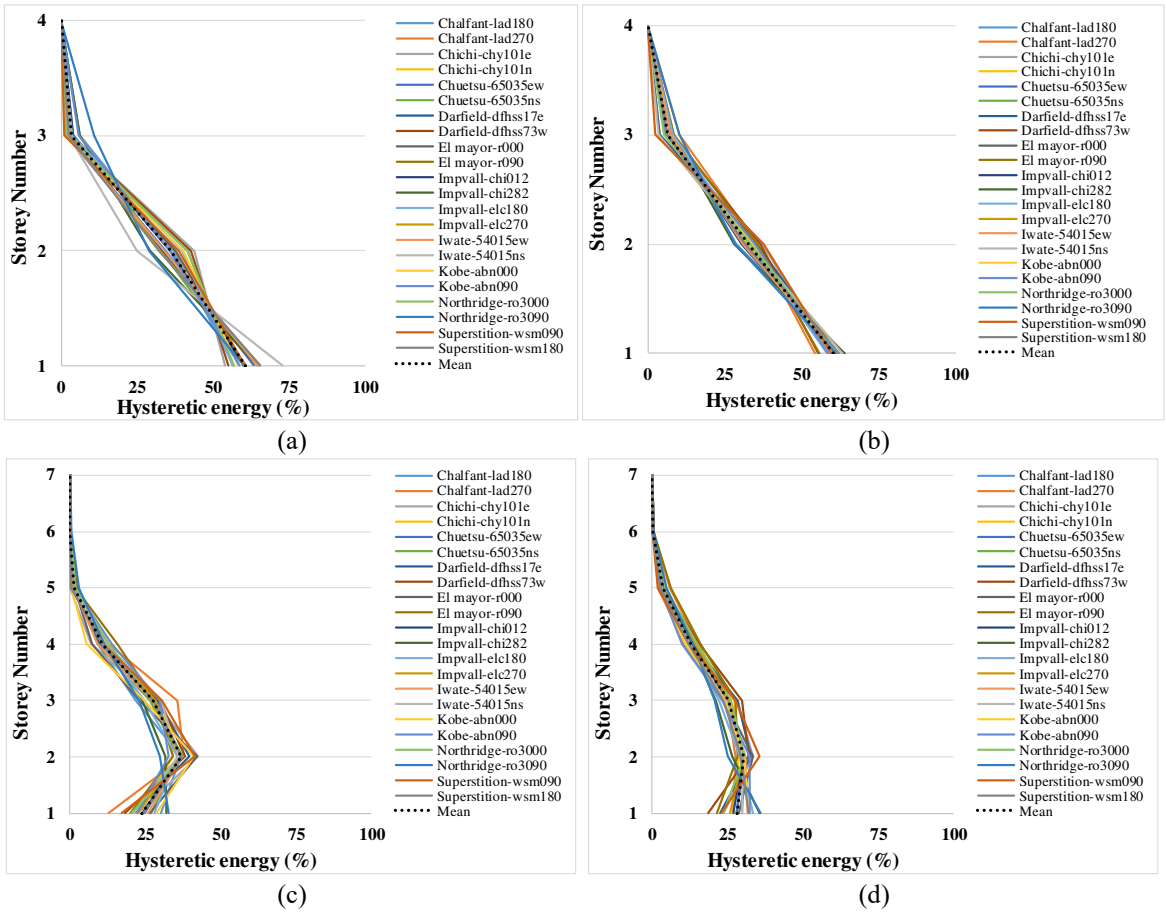

Fig. 8 Distribution of hysteretic energy to storeys: (a) in 4-storey model for DD-2, (b) DD-1 earthquake levels, (c) in 7-storey model for DD-2 and (d) DD-1 earthquake levels

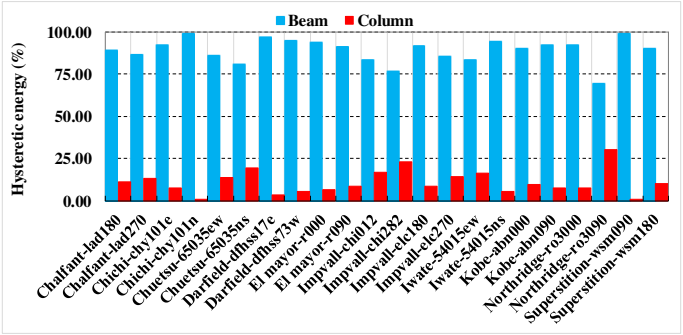

(a)

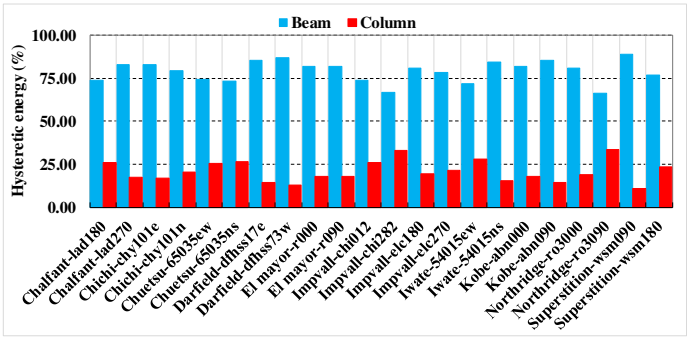

(b)

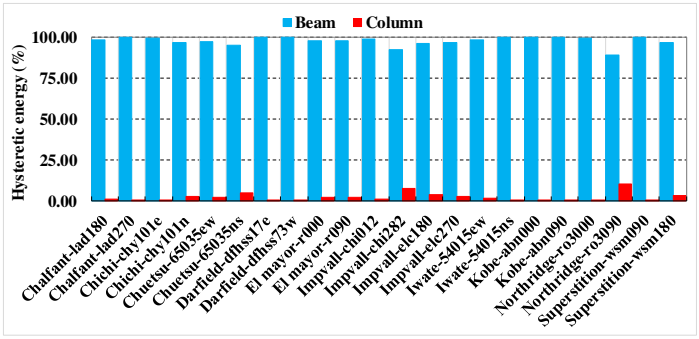

(c)

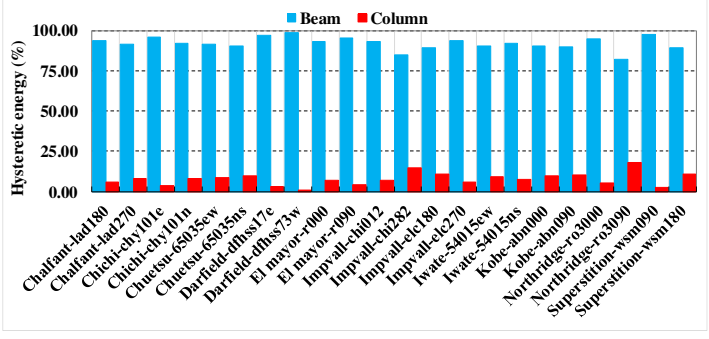

(d)

Fig. 9 Distribution of hysteretic energy to structural elements : (a) in 4-storey model for DD-2, (b) DD-1 records, (c) in 7-storey model for DD-2 and (d) DD-1 records

7.2 Relation between roof drift and input energy

Many researchers have conducted studies to determine the relationship between displacement and energy demands (Fabrizio et al. 2011; Hori and Inoue 2002; Ye and Otani 1999). For this purpose, the parameters for specific ductility and period intervals were calculated by using the energy and displacement values obtained from the analyzes of SDOF systems. Based on these parameters, various spectra were proposed by them. In the current study, comparisons of variables such as energy and displacement was carried out over four correlations: roof drifts (SDOF-MDOF), energy values (SDOF-MDOF) and roof drifts-energy values (separately for SDOF and MDOF). In order to evaluate the buildings as a whole, the percentage of these values is taken after the roof displacements are divided by building height and entitled as "roof drift ratio (%)", input energies are normalized by masses of buildings and entitled as "(E_I/m)[m^2/s^2]" (Fig. 10).

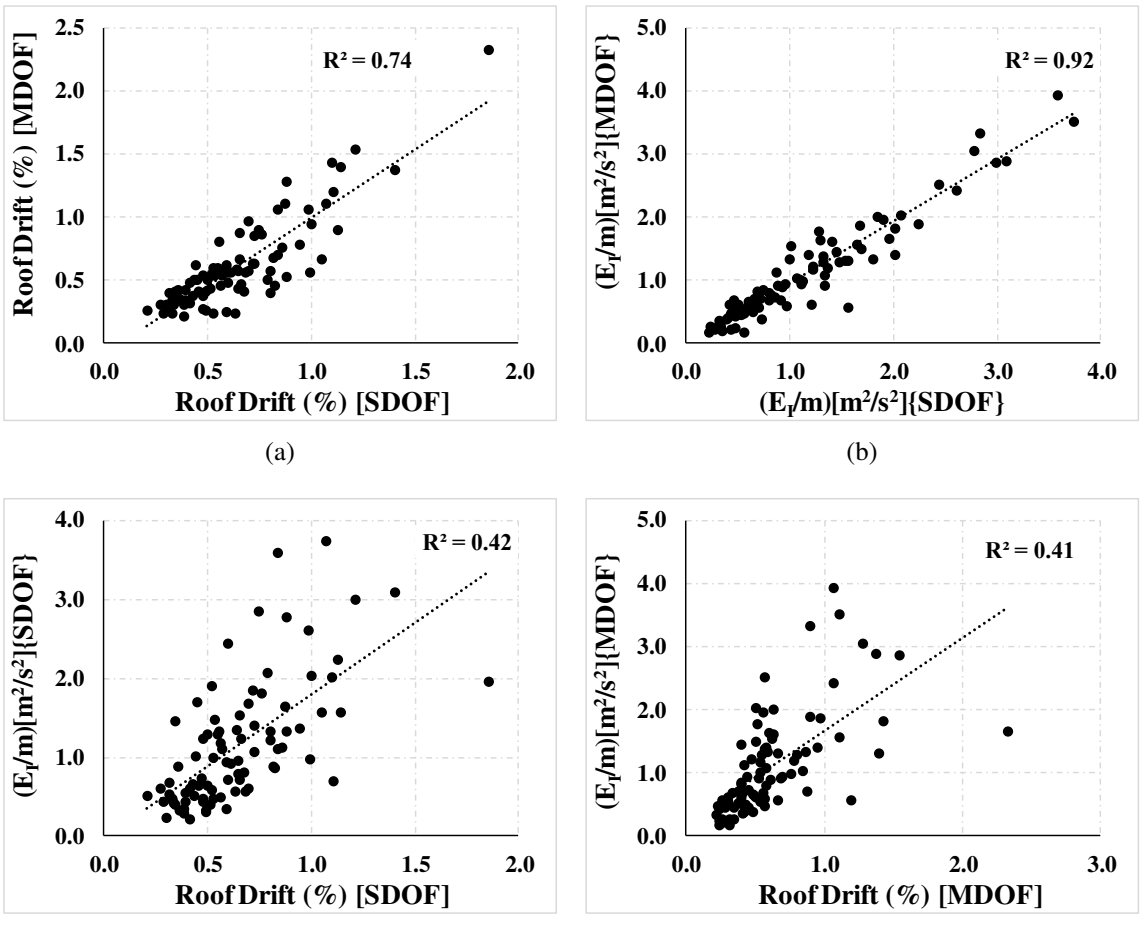

Fig. 10 The comparison of displacement and energy demands: (a) roof drifts, (b) input energies, (c) roof drifts- input energies for SDOF and (d) MDOF

The correlation between the input energy values obtained from the SDOF and MDOF is higher than the roof drifts. The relationship of roof drifts and input energy data is underestimated for both SDOF and MDOF systems. The medium correlation (approximately R≈0.65) between the energy and the drift values can be attributed to the cumulative calculation of the energy data, although the displacement values are obtained instantaneously.

8. Correlation between GMPs with input energy

8.1 Single parameter correlation

Evaluation of the damage status of the structures is carried out in two ways, before and after the earthquake. In the first case, the damage of the structure is determined analytically by seismic analysis methods, considering the dynamic properties of the structure and earthquake scenarios. In the second case, damage assessment of the building is made with rapid seismic assessment methods that take into account the observational determination of structural defects which affect the seismic performance of the building by street scans. While the first stage includes the damage estimation of the undamaged structure, the second stage covers the investigations after the damage has occurred, so if the structure is seismically inadequate, it may be too late for the second stage. Whichever parameter of the earthquake considered in this study is more related to the input energy will provide a preliminary idea about the estimation of the damage without calculation. At the same time, it is thought that the amount of damage will indicate the performance of the building against the earthquake and shed light on situations such as whether the building can be repaired and strengthened, if necessary, deciding to demolish the building.

The aim of the correlation of energy values and ground motion parameters (GMPs) in the current study is to determine the parameters that best reflect the potential damage that may occur under future earthquake hazard. For this purpose, the relationship between the considered parameters and the input energy is calculated with the correlation coefficients (R) and transferred to the table numerically. In addition, linear trend line and determination coefficient (R^2) are added on the sample graphs to have information about the variation of energy with the magnitudes of the parameters.

The separation of buildings as 4- and 7-storeys is to see the effects of mass and period on the energy-earthquake parameter relationship rather than the number of storeys. While the mass directly affects the energy demands, the period is also affected as it is dependent on the mass. Moreover, even if the buildings have different storeys, they may have the same mass and period due to the structural characteristics of the buildings. Within the scope of this study, the variation of these on the correlation is examined by providing diversity in terms of mass and period.

In order to combine the energy demands with different storeys, the energy values independent from the mass are determined by normalizing the input energy demands with the building mass. The relationship

between these energy data and GMPs has been transformed into a situation where all buildings can be evaluated only in terms of SDOF and MDOF systems. Then, the dual correlation values of SDOF and MDOF are converted into a single value in order to understand the difference between the parameters more clearly.

Correlation of the parameters with the energy demands of building models with different number of storeys, SDOF-MDOF systems and combination of all are given in Tables 7. Besides, parameters are given in 4 groups under the "Type" column as acceleration, velocity, frequency and displacement. The parameters in each group are listed from largest to smallest depending on the correlation coefficient in the last column where all are combined. Grouping of parameters is preferred in order to see clearly whether the parameters related to the same type are dominant compared to other types.

Table 7 Correlation coefficients (R) of parameters with input energy values of building models according to different cases

Type	Parameter	4-storey		7-storey		All Systems		All Buildings		All
		SDOF	MDOF	SDOF	MDOF	4-storey	7-storey	SDOF	MDOF	
Acceleration	I_a	0.885	0.901	0.856	0.818	0.891	0.835	0.871	0.856	0.863
	I_c	0.876	0.886	0.857	0.804	0.879	0.828	0.866	0.842	0.853
	A_{rms}	0.783	0.786	0.784	0.708	0.783	0.743	0.783	0.744	0.763
	SMA	0.735	0.737	0.741	0.646	0.734	0.690	0.737	0.688	0.712
	ASI	0.677	0.707	0.642	0.605	0.690	0.621	0.659	0.652	0.655
	EDA	0.669	0.666	0.693	0.590	0.666	0.637	0.680	0.625	0.652
	PGA	0.667	0.667	0.689	0.585	0.666	0.633	0.677	0.623	0.649
	A95	0.664	0.663	0.686	0.582	0.662	0.630	0.674	0.619	0.646
Velocity	VSI	0.886	0.825	0.920	0.845	0.854	0.879	0.902	0.834	0.867
	HI	0.846	0.770	0.900	0.787	0.807	0.839	0.871	0.777	0.823
	CAV	0.741	0.754	0.708	0.684	0.745	0.694	0.725	0.716	0.720
	SMV	0.606	0.552	0.662	0.509	0.578	0.581	0.632	0.528	0.579
	PGV	0.550	0.495	0.637	0.447	0.522	0.536	0.591	0.469	0.529
	V_{rms}	0.331	0.280	0.412	0.218	0.305	0.309	0.370	0.247	0.307
	SED	0.285	0.256	0.331	0.183	0.271	0.253	0.307	0.218	0.262
Frequency	T_p	0.371	0.374	0.303	0.477	0.372	0.394	0.338	0.427	0.383
	T_m	0.153	0.029	0.258	0.161	0.093	0.206	0.204	0.098	0.150
	V_{max}/A_{max}	-0.118	-0.178	-0.060	-0.158	-0.147	-0.112	-0.090	-0.167	-0.129
Disp.	PGD	0.158	0.124	0.219	0.076	0.141	0.144	0.187	0.099	0.142
	D_{rms}	0.151	0.119	0.215	0.071	0.135	0.139	0.182	0.093	0.137

The correlation coefficients of the parameters in the acceleration group for the 7-storey building are

calculated to be 5% lower than the 4-storey model. The biggest differences in terms of the number of storeys are obtained for T_m and V_{max} /A_{max}, while the results of other parameters are close to each other. From a modeling perspective, the correlation values of SDOF are approximately 20% higher than MDOF. Parameters related to acceleration and velocity (except V_{rms} and SED) are found to have higher correlation when compared to ones related to frequency and displacement.

I_a, I_c, A_{rms}, and SMA as acceleration-related parameters have the best values, while VSI, HI and CAV have a good correlation in the velocity group. They have correlation coefficients in the range from 0.7 to 0.9. While ASI, EDA, PGA, A95 exhibit moderate correlations in the acceleration group, similar results are found in the SMV and PGV parameters of the velocity group. According to the findings, it is possible to say that more parameters related to acceleration give good results compared to other groups.

In accordance with the nature of calculating the energy amount, the parameters obtained cumulatively by integral show generally good correlation, while the parameters calculated instantly demonstrate a moderate correlation. For the V_{rms} parameter, very low and good correlations were obtained by Riddell and Garcia (2001), Riddell (2007) for the 0.2 and 1 s periods of the SDOF system, respectively. Since the periods (0.50 and 0.67s) of the buildings in the present study are between the periods used by them, the low correlation values obtained are acceptable for the V_{rms}. Although the energy expression is mentioned in the SED parameter, the weak correlation with the input energy stands out as a very surprising result, contrary to expectation.

None of the displacement and frequency-related parameters have notable results. Although T_p is one step ahead in the frequency group, it shows a poor correlation. Unlike other parameters, V_{max}/A_{max} has a very low relationship in the reverse direction (negative correlation). It is not possible to use parameters such as T_m, V_{max}/A_{max}, PGD and D_{rms} alone as damage indicators.

Since it is difficult to make observations and comments on the figures about parameters with low correlation, the relationships of parameters that correlate better with input energy are shown in Fig. 11 and 12 through sample graphs. The increment in intensity of ground motion, increases both the amount of the energy used as damage measure (DM) and the value of earthquake parameters considered as intensity measure (IM). The increase in the energy and parameters caused by the earthquake does not change at the same rate as the intensity of ground motion. Therefore, it can be concluded that as the intensity of seismic excitations increases, the point data in the related graphs move away from the trend line and the correlation of the parameters considered decreases.

The distribution of I_a and VSI parameters which have the strongest correlation with energy, varies in a narrower range compared to other parameters. It is clearly seen in Fig. 11 and 12, as in Table 7, that the values of SDOF are compatible with MDOF ones and the data do not deviate much from each other.

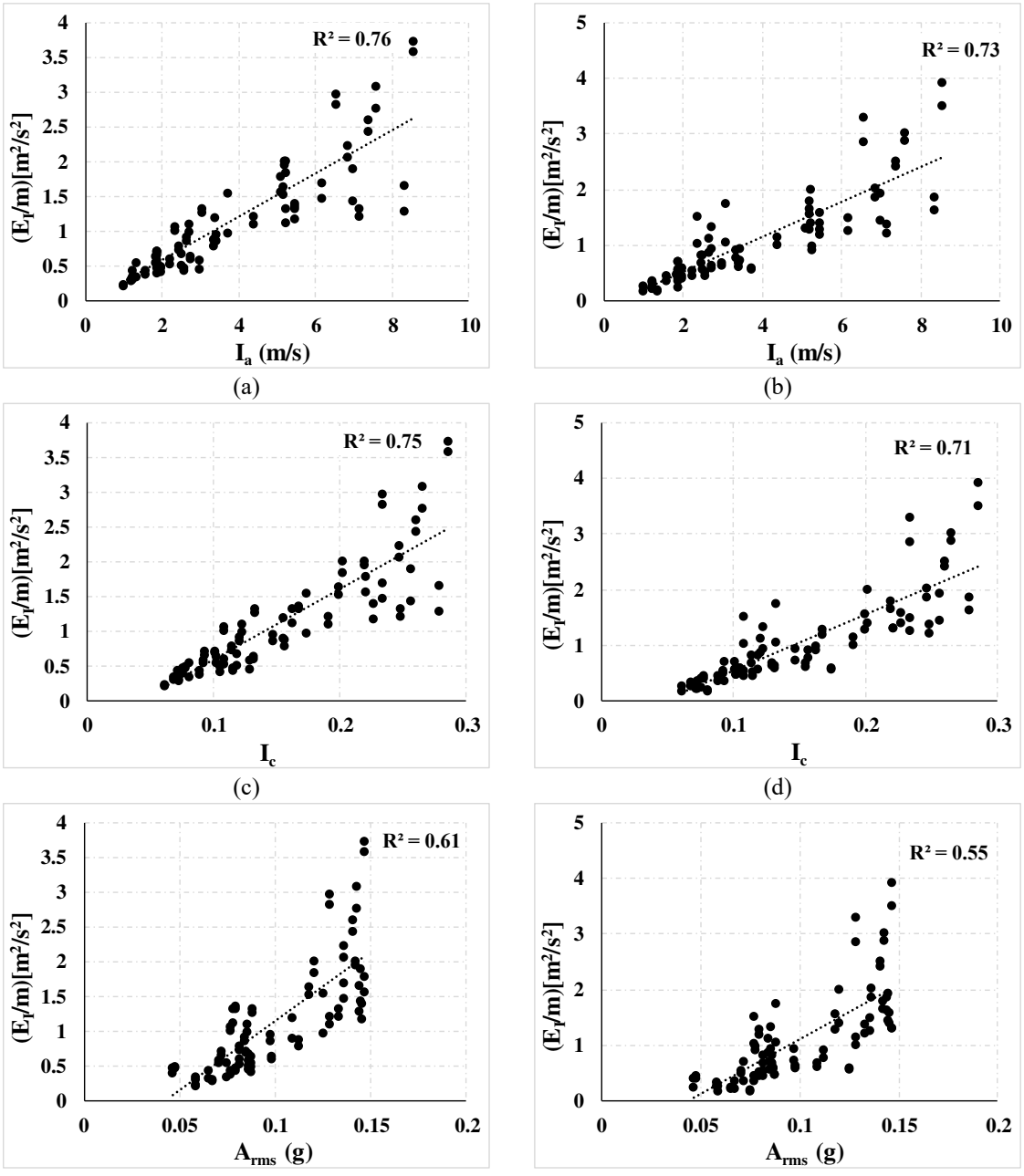

Fig. 11 Relation of some acceleration-related parameters with energy values for all buildings: left side for SDOF and right side for MDOF

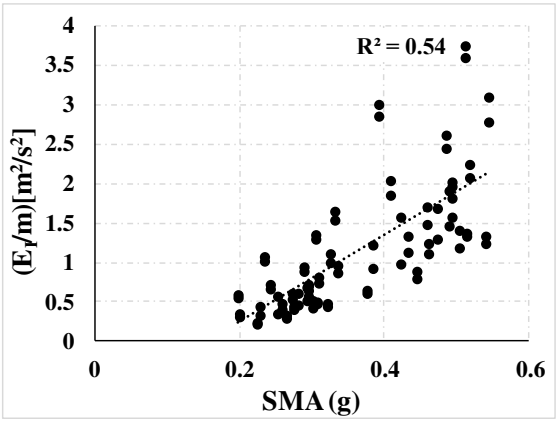

(g)

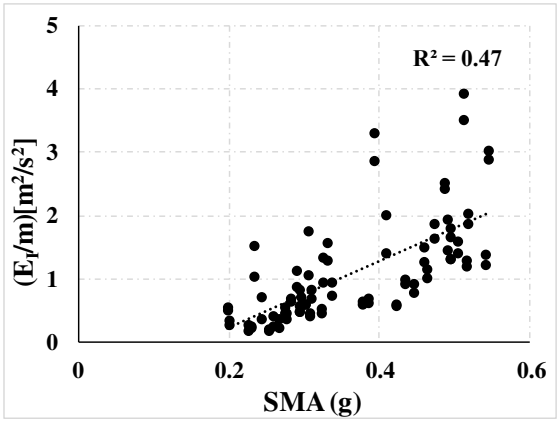

(h)

Fig. 11 Continued

575

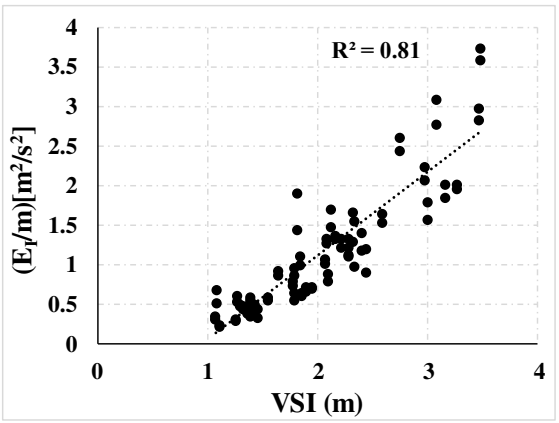

(a)

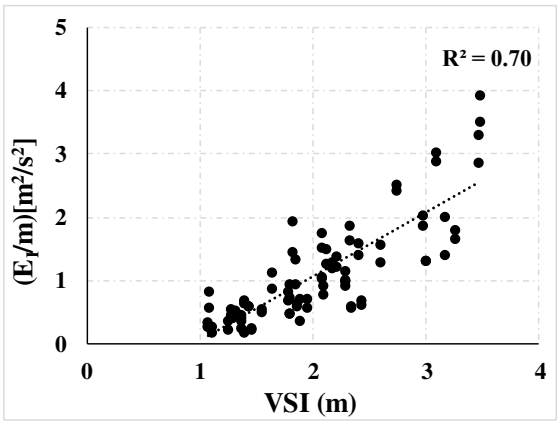

(b)

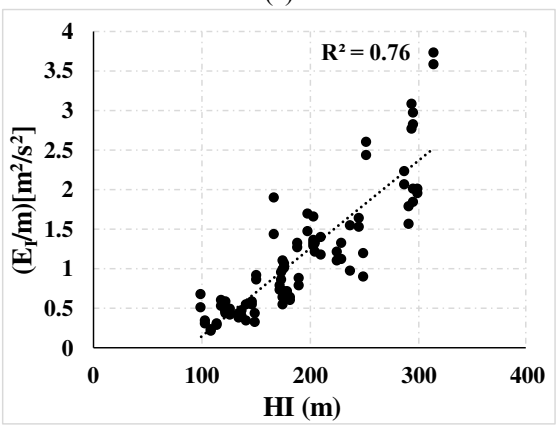

(c)

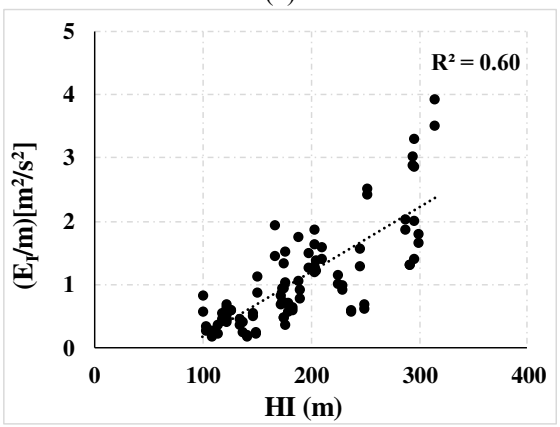

(d)

Fig. 12 Relation of some velocity-related parameters with energy values for all buildings: left side for SDOF and right side for MDOF

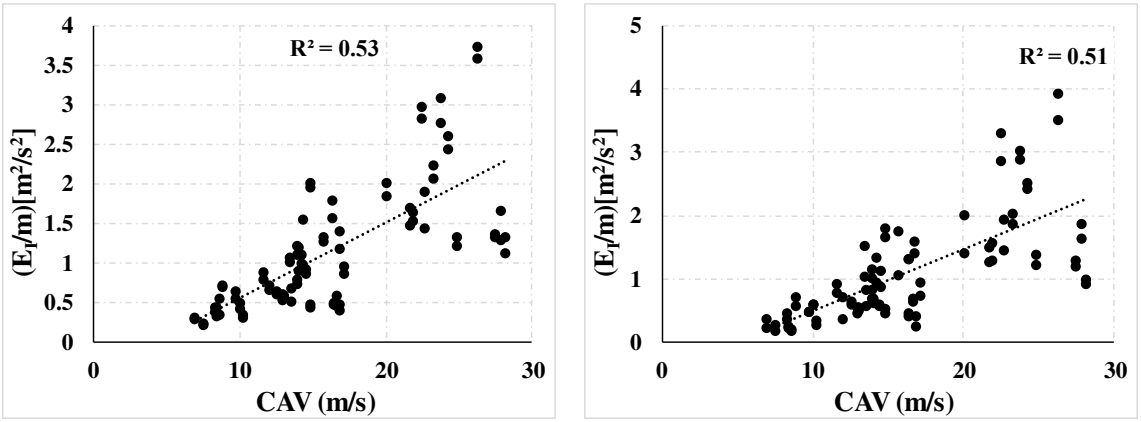

(d) (e)

Fig. 12 Continued

The R^2 values of the parameters are ranked in Fig. 13 by evaluating all buildings together in terms of SDOF and MDOF. Although the place of the parameters changes in arrangement, the parameter with low determination coefficient of SDOF does not have a high value for MDOF. Therefore, it can be concluded that SDOF and MDOF follow a parallel trend relative to each other.

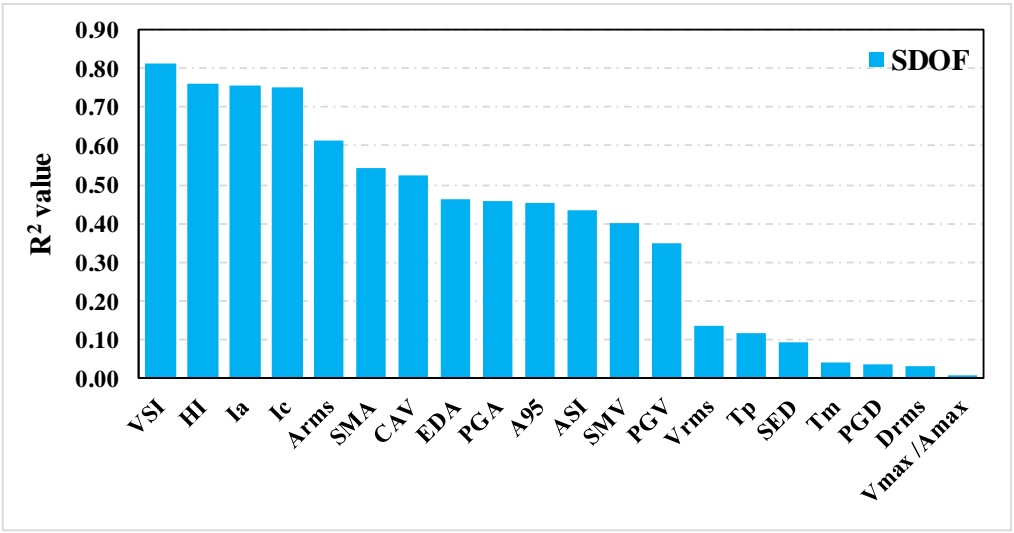

(a)

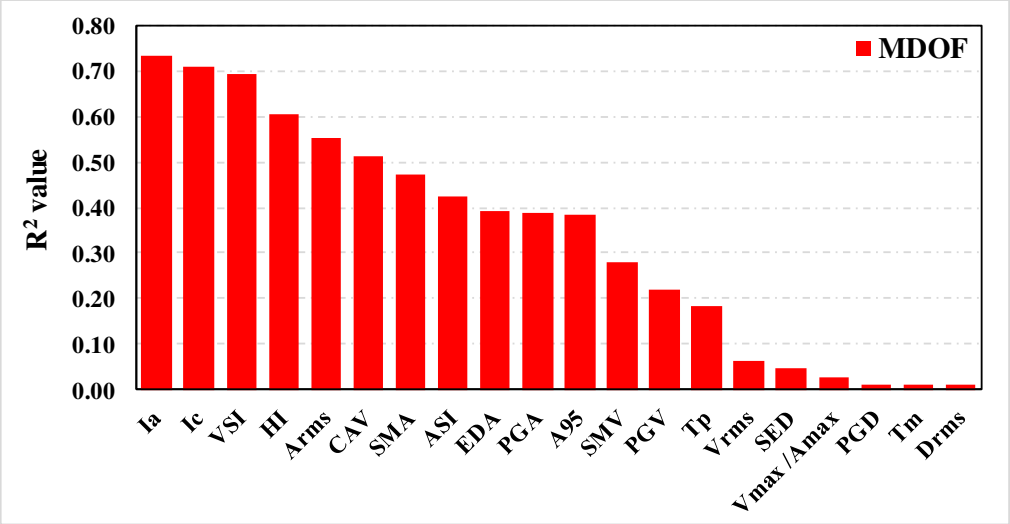

(b)

Fig. 13 R^2 values for GMPs of all models: (a) for SDOF and (b) MDOF systems

8.2 Multi parameter correlation

In order to increase the correlation obtained with the parameters within the scope of the study and to reduce the scattering, the case of using more than one parameter together instead of just one parameter was also examined. For this reason, different equations for SDOF and MDOF have been discussed to combine parameters. In order to find the equations, it is aimed to obtain the highest correlation by using the least number of parameters. As a result of linear regression analyzes performed for this purpose, Eq. 23 and 24 were derived separately for SDOF and MDOF, respectively.

In multiple regression analyzes, relevant equations with 6 and 5 parameters were created for SDOF and MDOF, respectively, according to conditions such as P-Value (Significance Value) <0.05 and VIF (Variance Inflation Factor) <10. When all of 20 GMPs are taken into account, the correlation coefficients are calculated as 0.981 and 0.975 for SDOF and MDOF, respectively, and these values are obtained as 0.945 and 0.937 via the equations (Fig. 14). Although there is a decrease of approximately 4% in the correlation coefficients obtained with the equations compared to all parameters, the energy amount can be easily calculated with fewer parameters by reducing the number of variables.

VSI and I_a parameters reflect the damage potential of earthquakes as the best single parameter for SDOF and MDOF, respectively. The correlation coefficients of these parameters were previously calculated as 0.902 and 0.856, and these values were improved with an increase of 5% and 10% thanks to multiple regression. It is noteworthy that although parameters such as PGV and D_{rms} do not have a high correlation on their own, they are included in the equations together with the VSI and I_a parameters.

$$E_I(m^2/s^2) = -1.088 - 1.012\,PGV + 7.61A_{rms} + 0.04283\,CAV - 1.793\,ASI + 0.8761\,VSI + 0.763A95 \quad (23)$$

$$E_I(m^2/s^2) = -0.629 - 1.636\,PGV + 0.1208\,D_{rms} + 0.2439\,I_a + 0.00628\,HI + 1.319\,T_p \quad (24)$$

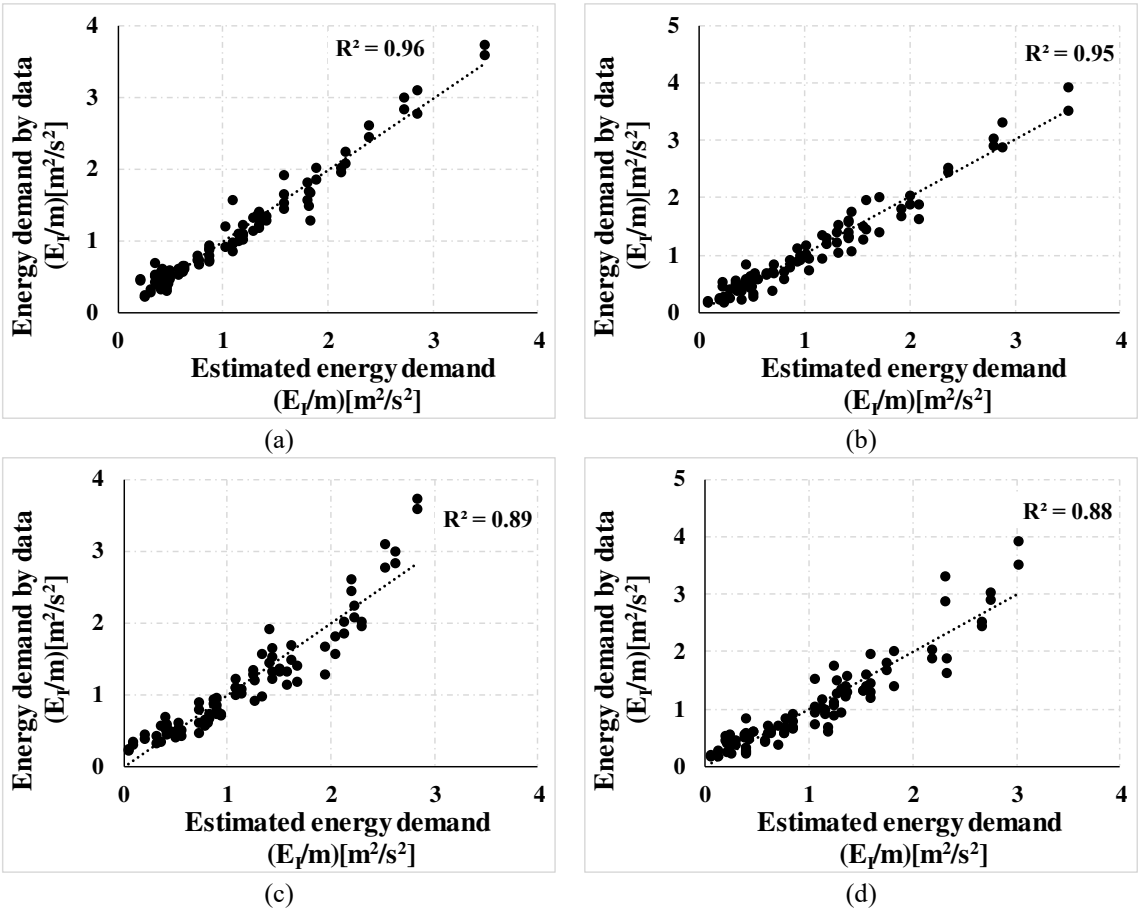

Fig. 14 The relationship between energy demands estimated by ground motion parameters and obtained from the analysis results: (a) for 20 GMPs with SDOF, (b) MDOF, (c) for selected parameters with SDOF and (d) MDOF

While the input energy estimation can be made through the generated equations, the amount of hysteretic energy can be calculated approximately by using the E_H/E_I ratios, which were previously found separately for SDOF and MDOF systems. While getting an idea about the amount of input energy with the equations used in the current study, it also shows that there is a significant relationship between the relevant parameters and

energy demands.

Since it aims to provide preliminary information about the correlation of the combined parameters and the energy amount with the created equations, many different equations can be derived with various assumptions and additional parameters. It should be kept in mind that the literature can be enriched by expanding the scope due to the proposed equations are limited to the models, the number of earthquakes and the parameter type in the study.

9. Conclusions

Seismic loads are crucial among the loads considered in the design of earthquake-resistant structures and evaluation of existing buildings. There are many studies highlighting the different properties of ground motion records to predict the response of structures under seismic loads. This study investigates the correlation of ground motion parameters (GMPs) with energy demands of low-rise reinforced concrete buildings without shear walls. For this purpose, 4- and 7-storey buildings without any irregularity are modeled to represent low-rise structures. In order to obtain the demands of SDOF systems as well as MDOF systems, the properties of "equivalent" SDOF systems are determined by using MDOF systems. For design and maximum earthquake levels, 44 ground motion records in total, 22 pairs in compliance with the Turkish Building Earthquake Code (TBEC 2018) are selected and scaled. The 20 GMPs depending on different variables (e.g. acceleration, velocity, displacement, and frequency) for each of the records are used within the scope of the study. Input energy data are considered as demand measure and these values are normalized with the masses of the buildings for cases where the buildings are evaluated together. The correlation of input energy results and GMPs is also investigated in terms of the number of storey and modeling. The correlation of 20 GMPs of 44 records with the energy demands obtained from a total of 176 nonlinear time history analyses is examined for the current study. The significant gains and outcomes within the scope of the study are summarized below:

- In the evaluation made on all earthquakes, the input energy values of the 4-storey model with SDOF are 10% higher than the MDOF, while the values of SDOF and MDOF for the 7-storey model are close to each other. In terms of the correlation coefficient, the SDOF values for all parameters are calculated as approximately 20% more than MDOF. Considering the amount of energy and correlation values, it can be said that MDOF is successfully represented by SDOF.
- While the biggest differences in terms of the number of storeys are calculated in the frequency-related T_m and V_{max} /A_{max} parameters, the correlation values of the 7-storey building are 5% lower than the 4-storey building for all acceleration-related parameters. It is observed that the results of the parameters in the other velocity and displacement groups are close to each other.
- It is possible to say that the parameters in the velocity (except V_{rms} and SED) and acceleration groups are

more dominant than the ones in the frequency and displacement groups because they have better correlations. On the other hand, it should be noted that both frequency and displacement-related parameters have low correlation values.

- Among the acceleration-related parameters, I_a, I_c, A_{rms}, and SMA have the strongest correlation, while VSI, HI, and CAV show the best correlation in the velocity group. The correlation coefficients of these parameters are greater than 0.70.
- I_a has the best correlation and the least scatter with energy demands for acceleration group parameters, which ensures it is the best parameter to reflect the damage potential of earthquakes. Similar results have also been obtained by Cao and Ronagh (2014), Ozmen and Inel (2016), and Yang et al. (2009).
- VSI is also good indicator as intensity measure and reflection of the potential damage. This consequence is also compatible with the studies by Yakut and Yılmaz (2008), Kostinakis et al. (2015), Massumi and Gholami (2016), and Kamal and Inel (2021).
- As well-known parameters, PGA and PGV show moderate correlation. This is also a parallel inference with Riddell and Garcia (2001), and Riddell (2007).
- In the current study, the T_m, V_{max}/A_{max}, PGD and D_{rms} parameters do not appear to be useful indicators of damage alone. Lowest correlations of these parameters have been emphasized by Cao and Ronagh (2014), and Ozmen and Inel (2016).
- This paper also investigated combining multiple ground motion parameters using multiple regression to reflect damage potential better than a single parameter. Thanks to the equations proposed for SDOF and MDOF systems via multiple regression, the correlation coefficients are increased to 0.945 and 0.937 with an increase of 5% and 10%, respectively.
- In addition to damage measures such as various damage indexes, interstorey and roof drift ratios, it is concluded that input energy as highlighted in previous studies can also be used according to the findings in the present study.

In order to obtain better correlation results, demands such as displacement and energy should be estimated correctly. For this reason, modeling of structures is indispensable properly. The period of created buildings in the regions like short, intermediate and long periods also affects the behavior of the structure against earthquakes. Especially in the long period region, the stability of the spectral accelerations in the response spectrum of the earthquakes ensures that the demands of the structures in this region are close to each other. This can increase the correlation of their demands with considered the earthquake parameters. The choice of variables such as displacement and energy as demand measures affects the degree of correlation. Different variables (e.g. acceleration, velocity, displacement, and frequency) used in the calculation of ground motion

parameters may be decisive in the correlation success. In addition, the relationship between parameters and demands is also influenced by the usage of regression types such as linear or nonlinear regression.

Declarations

Funding Author declares that no funds, grants, or other support were received during the preparation of this manuscript.

Conflict of interest Author has no conflict of interest with others and third parties for current manuscript.

References

Akkar S, Özen Ö (2005) Effect of peak ground velocity on deformation demands for SDOF systems. Earthq Eng Struct Dyn 34: 1551–1571. https://doi.org/10.1002/eqe.492

Arias A (1970) Measure of earthquake intensity. Massachusetts Inst of Tech, Cambridge Univ of Chile, Santiago de Chile 438–483.

ASCE 41-13 (2014). Seismic evaluation and retrofit of existing buildings, American Society of Civil Engineers, USA.

ATC-40 (1996) Applied Technology Council, seismic evaluation and retrofit of concrete buildings, California Seismic Safety Commission; California, USA.

Benavent-Climent A, López-Almansa F, Bravo-González DA (2010) Design energy input spectra for moderate-to-high seismicity regions based on Colombian earthquakes. Soil Dyn Earthq Eng 30: 1129–1148. https://doi.org/10.1016/j.soildyn.2010.04.022

Cabanas L, Benito B, Herraiz M (1997) An approach to the measurement of the potential structural. Earthq Eng Struct Dyn 26: 79–92.

Cao V Van, Ronagh HR (2014) Correlation between seismic parameters of far-fault motions and damage indices of low-rise reinforced concrete frames. Soil Dyn Earthq Eng 66: 102–112. https://doi.org/10.1016/j.soildyn.2014.06.020

Dindar AA, Yalçin C, Yüksel E, Özkaynak H, Büyüköztürk O (2015) Development of earthquake energy demand spectra. Earthq Spectra 31: 1667–1689. https://doi.org/10.1193/011212EQS010M

Elenas A (2000) Correlation between seismic accelaration parameters and overall structural damage indices of buildings. Soil Dyn Earthq Eng 20: 93–100. https://doi.org/10.1016/S0267-7261(00)00041-5

Elenas A (1997) Interdependency between seismic acceleration parameters and the behaviour of structures. Soil Dyn Earthq Eng 16: 317–322. https://doi.org/10.1016/S0267-7261(97)00005-5

Elenas A, Meskouris K (2001) Correlation study between seismic acceleration parameters and damage indices of structures. Eng Struct 23: 698–704. https://doi.org/10.1016/S0141-0296(00)00074-2

Fabrizio M, Bruno S, Decanini L, Saragoni R (2011) Correlations between energy and displacement demands for performance-based seismic engineering. Pure Appl Geophys 168: 237–259. https://doi.org/10.1007/s00024-010-0118-9

Fahjan YM (2008) Selection and scaling of real earthquake accelerograms to fit the Turkish design spectra. Tech J Turkish Chamb Civ Eng 19: 4423–4444.

Fajfar P, Vidic T (1994) Consistent inelastic design spectra: Hysteretic and input energy. Earthq Eng Struct Dyn 23: 523–537. https://doi.org/10.1002/eqe.4290230505

FEMA-356 (2000) Federal Emergency Management Agency, Prestandard and commentary for the seismic rehabilitation of buildings, American Society of Civil Engineers (ASCE); Washington, USA.

Hori N, Inoue N (2002) Damaging properties of ground motions and prediction of maximum response of structures based on momentary energy response. Earthq Eng Struct Dyn 31: 1657–1679. https://doi.org/10.1002/eqe.183

Housner GW (1952) Spectrum intensities of strong-motion earthquakes. Symp Earthq Blast Eff Struct 20–36.

Kamal M, Inel M (2021) Correlation between ground motion parameters and displacement demands of mid-rise rc buildings on soft soils considering soil-structure-interaction. Buildings 11(3):125. https://doi.org/10.3390/buildings11030125

Khashaee P, Mohraz B, Sadek F, Lew HS, Gross JL (2003) Distribution of earthquake input energy in structures. National Institute of Standards and Technology, Gaithersburg, USA.

Koç G (2017) Effects of ground motion characteristics on structural energy response of buildings. MSc Thesis, Istanbul Technical University.

Kostinakis K, Athanatopoulou A, Morfidis K (2015) Correlation between ground motion intensity measures and seismic damage of 3D R/C buildings. Eng Struct 82: 151–167. https://doi.org/10.1016/j.engstruct.2014.10.035

Kramer SL (1996) Geotechnical earthquake engineering. Prentice- Hall, Upper Saddle River, NJ, USA.

Liao WI, Loh CH, Wan S (2001) Earthquake responses of RC moment frames subjected to near-fault ground motions. Struct Des Tall Build. 10: 219–229. https://doi.org/10.1002/tal.178

Mander JB, Priestley MJN, Park R (1988) Theoretical stress-strain model for confined concrete. J Struct Eng 114: 1804–1826. https://doi.org/10.1061/(asce)0733-9445(1988)114:8(1804)

Massumi A, Gholami F (2016) The influence of seismic intensity parameters on structural damage of RC buildings using principal components analysis. Appl Math Model 40: 2161–2176. https://doi.org/10.1016/j.apm.2015.09.043

Merter O (2019) An investigation on the maximum earthquake input energy for elastic SDOF systems. Earthq Struct 16: 487–499. https://doi.org/10.12989/eas.2019.16.4.487

Nuttli OW (1979) The relation of sustained maximum ground acceleration and velocity to earthquake intensity

741 and magnitude. US Army Engineer Waterways Experiment Station.
742 Okur A, Erberik MA (2014) Adaptation of energy principles in seismic design of Turkish RC frame structures.
743 Part II: Distribution of Hysteretic Energy, 15th World Conference on Earthquake Engineering
744 (15WCEE). Istanbul: 1–11.
745 Ozmen HB, Inel M (2016) Damage potential of earthquake records for RC building stock. Earthq Struct 10:
746 1315–1330. https://doi.org/10.12989/eas.2016.10.6.1315
747 Palanci M, Senel SM (2019) Correlation of earthquake intensity measures and spectral displacement demands
748 in building type structures. Soil Dyn Earthq Eng 121: 306–326.
749 https://doi.org/10.1016/j.soildyn.2019.03.023
750 PEER (2019) Pacific Earthquake Engineering Research Center; Berkeley University, California, USA.
751 https://ngawest2.berkeley.edu/
752 Rathje EM, Abrahamson NA, Bray JD (1998) Simplified frequency content estimates of earthquake ground
753 motions. J Geotech Geoenvironmental Eng 124: 150–159.
754 Reed JW, Anderson N, Chokshi NC, Kennedy RP, Metevia WJ, Ostrom DK, Stevenson JD (1988) A criterion
755 for determining exceedance of the operating basis earthquake: Final report.
756 Riddell R (2007) On ground motion intensity indices. Earthq Spectra 23: 147–173.
757 https://doi.org/10.1193/1.2424748
758 Riddell R, Garcia JE (2001) Hysteretic energy spectrum and damage control. Earthq Eng Struct Dyn 30: 1791–
759 1816. https://doi.org/10.1002/eqe.93
760 SAP2000 (2018) Integrated finite element analysis and design of structures basic analysis reference manual.
761 Computers and Structures Inc, Berkeley, USA.
762 Sarma SK, Yang KS (1987) An evaluation of strong motion records and a new parameter A95. Earthq Eng
763 Struct Dyn 15: 119–132. https://doi.org/10.1002/eqe.4290150109
764 SeismoSignal (2022) A computer program for processing of strong-motion data. Earthquake Engineering
765 Solutions.
766 Sucuoğlu H, Nurtuğ A (1995) Earthquake ground motion characteristics and seismic energy dissipation. Earthq
767 Eng Struct Dyn 24: 1195–1213. https://doi.org/10.1002/eqe.4290240903
768 Sucuoğlu H, Yücemen S, Gezer A, Erberik A (1998) Statistical evaluation of the damage potential of
769 earthquake ground motions. Struct Saf 20: 357–378. https://doi.org/10.1016/S0167-4730(98)00018-6
770 TBEC 2018 (2018) Turkish Building Earthquake Code. Republic of Turkey Ministry of Interior Disaster and
771 Emergency Management Presidency: Ankara, Turkey.
772 Travasarou T, Bray JD, Abrahamson NA (2003) Empirical attenuation relationship for Arias Intensity. Earthq
773 Eng Struct Dyn 32: 1133–1155. https://doi.org/10.1002/eqe.270
774 Von Thun JL, Roehm LH, Scott GA, Wilson JA (1988) Earthquake ground motions for design and analysis of

dams, iEarthquake Engineering and Soil Dynamics II—Recent Advances in Ground-Motion Evaluation: 463–481.

Yakut A, Yılmaz H (2008) Correlation of deformation demands with ground motion intensity. J Struct Eng 134: 1818–1828. https://doi.org/10.1061/(asce)0733-9445(2008)134:12(1818)

Yang D, Pan J, Li G (2009) Non-structure-specific intensity measure parameters and characteristic period of near-fault ground motions. Earthq Eng Struct Dyn 38:1257–1280. https://doi.org/10.1002/eqe.889

Ye L, Otani S (1999) Maximum seismic displacement of inelastic systems based on energy concept. Earthq Eng Struct Dyn 1499: 1483–1499.

Zhu TJ, Tso WK, Heidebrecht AC (1988) Effect of peak ground a/v ratio on structural damage. J Struct Eng 114: 1019–1037. https://doi.org/10.1061/(asce)0733-9445(1988)114:5(1019)

Supplementary Files

This is a list of supplementary files associated with this preprint. Click to download.

- Highlights.docx